An autonomous time dependent swarm routing system for UAV real time investigation

Kyriacos Antoniades[1], Alessio Ishizaka, Jana Ries

Icarus and Daedalus, 24 Regent Trade Park,
Barwell Lane, Gosport, PO13 0EQ, UK
www.icarus-daedalus.co.uk

Abstract - This paper implements an autonomous time dependent swarm routing system for navigating a set of unmanned aerial vehicles (UAVs) aka drones, to investigate a set of maritime vehicles (MVs) in an area of interest (AOI). The autonomous routing system integrates two multi criteria decision analysis (MCDA) methodologies, namely the analytic hierarchy process AHP and PROMETHEE, a geographical information system (GIS) and a mathematical programming (MP) technique. The order of the MV investigation is based on their degree of "suspiciousness", providing an innovative step toward intelligent swarm of UAVs operating in a coordinated and coupled fashion to achieve multiple MV investigation, managed by a single operator. This system provides first notions towards intelligent and fully autonomous UAVs. The updated functionality of this decision support system, with a combined drug trafficking and illegal immigration scene assessment case study is presented. To the best of our knowledge, a real-time dynamic autonomous routing problem has not yet been solved, especially a swarm routing one. This is our original contribution, the methods used are well-known; but their integration to solve this problem is unique. The hybrid set-up and use of MCDA techniques facilitate the translation of surveillance expert knowledge into an advanced and automated decision support tool.

Keywords – Cognitive Autonomy, Moving Target TSP, Dynamic VRP, AHP, PROMETHEE, GIS, Mathematical Programming, OR in Defence

[1] kyriacos.antoniades@icarus-daedalus.co.uk

1. Introduction

The “Future of drone use” article [1], distinguishes different types of drones that can be differentiated in terms of the type, the degree of autonomy, the size and weight, and the power source. Drones will become increasingly autonomous and more capable of operating in swarms. Some of the widely-used existing commercial Unmanned Air Systems (UAS) drone models and their overview characteristics can be shown in Figure 1.

Characteristics	Delfly Explorer	Hubsan x4 Drone	Parrot A.R. Drone	DJI Phantom	Raven	ScanEagle
Type of drone						
Fixed-wing	-	-	-	-	X	X
Multirotor	-	X	X	X	-	-
Other	X	-	-	-	-	-
Autonomy						
Human operated system	-	X	X	X	X	X
Human delegated system	-	-	X	X	X	X
Human supervised system	X	-	-	-	-	-
Fully autonomous system	-	-	-	-	-	-
Size/weight						
Large drone (25-150 kg)	-	-	-	-	-	-
Small drone (2-25 kg)	-	-	-	-	X	X
Mini drone (up to 2 kg)	X	X	X	X	-	-
Energy source						
Airplane fuel	-	-	-	-	-	X
Battery cells	X	X	X	X	X	-
Fuel cells	-	-	-	-	-	-
Solar cells	-	-	-	-	X	-

Figure 1. Overview characteristics

According to the definition by the International Organization for Standardization (ISO), robot autonomy is the ability to perform intended tasks based on current state and sensing, without human intervention [2]. This definition encompasses a wide range of situations, which demand different levels of autonomy depending on the type of robot and the intended use. In the case of small drones, three levels of increasing autonomy can be identified as seen on Table 1 [3].

	Exteroceptive sensors	Computational load	Supervision required	Readiness level	Drone type
Sensory-motor autonomy	None or few	Little	Yes	Deployed	All types
Reactive autonomy	Few and sparse	Medium	Little	Partly deployed	Fixed wing, rotorcraft and flapping wing
Cognitive autonomy	Several and high density	High	None	Not yet deployed	Mostly rotorcraft

Table 1. Levels of autonomy: requirements, availability and readiness for market

1. Cognitive autonomy (requires reactive autonomy): perform simultaneous localization and mapping; resolve conflicting information; plan (for battery recharge for example); recognize objects or persons; learn.
2. Reactive autonomy (requires sensory-motor autonomy): maintain current position or trajectory in the presence of external perturbations, such as wind or electro-mechanical failure; avoid obstacles; maintain a safe or predefined distance from ground; coordinate with moving objects, including other drones; take off and land
3. Sensory-motor autonomy: translate high-level human commands (such as to reach a given altitude, perform circular trajectory, move to global positioning system (GPS) coordinates or maintain position) into combinations of platform-dependent control signals (such as pitch, roll, yaw angles or speed); follow pre-programmed trajectory using GPS waypoints.

UAVs used in our case study, are not autonomous as they are piloted remotely from the ground control station following the indications of at least two human operators. The aim of this study is to increase further the autonomy of UAVs by developing a real-time decision support system that will automate a UAV's navigation path for maritime surveillance, based on MVs *suspiciousness*. In this highly dynamic and uncertain environment, traditional optimization routing vehicle algorithms cannot be used. The decision support system

indicates to a UAV at any interval of time, which MV out of the set is ranked as the most *suspicious* and therefore be of higher priority to be immediately investigated. This means that the urgency of the local priority is much more important than the overall efficiency. To solve this problem, four methods have been used in combination. These include:

1. AHP (Analytic Hierarchy Process)
2. PROMETHEE (Preference Ranking Organization METhod for Enrichment Evaluation)
3. MP (Mathematical Programming)
4. GIS (Geographical Information System)

The ranking of suspicious MVs depends on the mission (e.g. drug trafficking, illegal immigration, etc), defined as mission criteria. For each mission, a set of suspiciousness indicators are defined (e.g. speed of the MV, size, etc). These are called target sub-criteria of the mission criteria. To obtain the overall *criteria weights (suspiciousness)*, a criteria hierarchy has been constructed (Section 4.2), weighted (Section 4.3, Section 4.4) and calculated (Section 4.5) with AHP. This activity can be planned as an a priori and recorded for later a posteriori utilisation. The overall *criteria weights* are then reported to all UAVs, which rank at every interval of time a set of simultaneously targeted MVs (Section 4.6) based on their *suspiciousness*. The automatic identification system (AIS) provides real time locations of all UAVs and MVs. This information is also used to calculate the location of MVs at any time *t*. The routing of the UAV is then adapted in real time to reach the predicted location of the MV at time t+1. The geographical information system (GIS) provides the global real-time view of the running scenario of operation and further performance analysis of a surveillance mission (Section 4.7). Finally, in the case of two or more UAVs ranking equally for the same MV to be investigated, a mathematical programming method can be used to break the tie to uniquely assig a UAV to a specific MV, by maximising the PROMETHEE net flows (Section 4.8). Details of the above-mentioned methodologies are discussed further in the succeeding sections. The structure of the paper is as follows. Section 2 discusses current methods used in UAV navigation and how multi-criteria decision analysis (MCDA) methods have been used in various fields in the defence sector, particularly observing a gap in MCDA utilization for UAV navigation. Section 3 describes the proposed solution combining the four methods as described above. Section 4 illustrates a case study, followed by the conclusions in Section 5.

2. Literature review

Drone routing can be modelled as a vehicle routing problem (VRP) which was introduced by Dantzig and Ramser [4] as a generalization of the classic Travelling Salesman Problem (TSP). It is defined as the search for a set of routes from one or several depots passing through a set of cities exactly once, while minimizing total cost [5]. A vast number of extensions to the classic VRP has been introduced in recent years, including the consideration of capacity constraints, time windows, fleet characteristics and pick-up/delivery scenarios. An overview can be found in [6]. Pillac, Gendreau [7] outlined the importance of two key components in real-life applications that are often omitted in the classic target routing problem: namely evolution and quality of information. The authors introduce an overview of the variety of dynamic target routing problems distinguishing between different deterministic and stochastic knowledge of input data and the difference in availability of input data. Braekers, Ramaekers [6] point out that most the VRP literature considers deterministic quality of information, with only a minority addressing stochastic or real-time information (9.17% and 4.59%, respectively). They further outline that there are no standard problem definitions available for dynamic VRPs, although the general focus leads to the uncertainty of customer requests, with the potential of stochastic information or forecasts being available.

		Information Quality	
		Deterministic knowledge of input data	**Stochastic knowledge of input data**
Information Evolution	**Input is known beforehand**	***Static Deterministic***	***Static Stochastic***
	Input changes over time	***Dynamic Deterministic***	***Dynamic Stochastic***

Table 2. Taxonomy of dynamic target problems

Various solutions addressing all four classes outlined in the taxonomy [8] in Table 2 have been proposed to route drone in the literature. Enright, Savla, Frazzoli, Bullo [9] discuss the problem in form of a dynamic stochastic problem where targets are generated based on a

Poisson process with the aim to minimize waiting time between the appearance and the observation of a target. The authors suggest a Dubbin's distance based approach which accounts for target dynamics. Russell and Lamont [10] discuss the need for a priori routing schedules and their amendment subject to real-time changes of the information using a fast-new coding structure for the Genetic Algorithm.

Several authors have addressed drone routing as a static and deterministic problem. Shetty, Sudit [11] considered Unmanned Combat Aerial targets where target information was known. The authors propose a Taboo Search heuristic to address the problem in two stages, namely target assignment and target routing. Jacobson, McLay [12] consider multiple search platforms when designing search strategies. They consider a formulation of the multiple TSP problem with no evolution of information using a generalized hill climbing algorithm. Kinney, Hill [13] and Harder, Hill [14] suggest a Taboo Search based approach for static and deterministic drone routing.

Liu, Zheng [15] consider a dynamic and stochastic modelling of drone routing by addressing the real- time path planning problem aiming to overcome potential obstacles in a hostile environment accounting for the impact on a drone's performance. The authors use a bi-level programming formulation to solve the problem. Edison and Shima [16] and Kuroki, Young [17] both present a Genetic Algorithm approach to a drone routing using multiple task assignment and path planning. Like the classes of dynamic target routing problems, the literature in dynamic and deterministic target routing problems focusses mainly on providing fast solution strategies to re-optimize the routing at different points of time based on significant dynamic changes in the environment. Ruz, Arevalo [18] and Berger, Boukhtouta [19] consider the use of Mixed integer linear programming (MILP) to find optimal drone trajectories. Duan, Zhang [20] and Lamont, Slear [21] present a Genetic Algorithm solving approach to the drone path planning.

Le Ny, Dahleh, Feron [22] introduce an approach using the concept of Monte Carlo simulation, modelling an independent two-state Markov chain for each target. When visiting a target, a drone receives a reward depending on its current state. The approach is demonstrated on a given set of targets. A concise literature review on the routing

optimization methods can be found by Alotaibi [23], whom used two integer linear methodologies for routing drone in the presence of threats.

Most algorithms for the dynamic VRP require re-optimization to account for dynamic changes, with further challenges being imposed by the need for real-life constraints. Moreover, in some cases it requires extensive expert knowledge about the problem, for instance in the form of simulation studies. In the case of the presented problem of scene assessment, it is important to note that the main priority of assigning a drone to a target at a point of time should be made based on the potential for highest gain to be rewarded in the form of detecting suspicious behaviour.

Real time vehicle solutions, their algorithms, parallel computing algorithms [24] describing a moving target travelling salesman problem (TSP) [25] are presented early as 2003. A decade later, the moving target – TSP is solved using genetic algorithms [26] and improved with trajectory projection [27] . A year on, it is solved using tree search and macro-actions [28]. Other methodologies include ant colony algorithms [29], [30], hybrid metaheuristic approach [31], in a continuous search space [32], [33], neighbourhood search algorithm [34], time windows [35], even used in controlled airspace [36].

Hence, the incorporation of a global optimization strategy by modelling drone routing as a VRP or DVRP would potentially sacrifice the rewarded gain at a given point of time in favour of global optimality of the route.

To avoid the latter, this report introduces the concept of multiple MCDA method solution as a novel strategy in assigning drone to targets in sea scene assessment, by allowing to determine the target to be investigated next by assessing its degree of suspicious behaviour relative to all other targets. Strictly speaking, the elements of MCDA is the combination of the technical approach and the social environment / processes that support it, with the latter being more important.

The problem of drone routing for sea surveillance is thence considered a dynamic and deterministic problem, given that the information on targets is of deterministic nature and made available in real-time. Consequently, optimized solutions can only be determined a-

posteriori. Proposed approaches have been to optimize at a given point of time which requires very fast solutions approaches, usually of heuristic nature.

A first application of single MCDA method to solving routing multi-objective problems can be observed by Zak [37], concerned about the acceptance or rejection of incoming orders based on the definition of minimum price for the orders and the assignment of targets to orders. This was solved using the ELECTRE III method. Similarly, the AHP method was used to a routing problem as carried out by Tavana [38]. The purpose was the assignment of aerial targets to mission packages on four competing objectives. Soon after, Tavana and Bourgeois [65] improved on the operational planning and navigation of autonomous underwater targets by utilizing ANP together with fuzzy sets. AHP was also used to estimate optimal path for road network [39] and finding optimum neighbourhood for routing [40].

One of the first multi MCDA methods is proposed by Macharis [41] involving AHP integration with PROMETHEE and discussing synergies between them in how PROMETHEE can be improved by adding a modularized AHP weighting system and conversely, when we replicate the AHP weighing approach in a PROMETHEE context then the decision maker needs to perform only a limited number of pairwise comparisons and is not dependent on the requirements of a scale system (i.e. Saaty's 1-9 scale).

Since then, there has been an increase of multi MCDA synergies as shown by Ho, Ishizaka and Labib [42], [43]. Single methods seem insufficient to provide an effective and realistic analysis of complex situations due to its inherent assumptions. Ries and Ishizaka [44]initially proposed a multi-MCDA (AHP-PROMETHEE) method to attempt to solve a real-time routing problem of drones within the context of sea scene assessment.

More recently, as far as autonomous routing is concerned, Jaishankar and Pralhad [45] develops an autonomous routing system for UAVs based on MCDA integration with GIS coupled with a distance transform technique. A combination of AHP and TOPSIS was presented by Yilmaz and Aplak [46] as a solution method for assessing alternative routes for a VRP. Dedemen [47] used AHP with PROMETHEE and GIS for the route selection of overhead power lines. Saini and Kumar [48] used AHP with fuzzy TOPSIS selection of best and most reliable route and provide alternative options for making a robust Mobile Ad-hoc

network. Ferreira, Costa, Tereso and Oliveira [49] presented a multi MCDA method for route planning of vehicles performing waste collection for recycling, based on AHP, SMART and Value Fn. Bandyopadhyay and Chanda [50] together with Bandni and Matrayee [51] used the Tarantula mating based multi-agent routing strategy together with PROMETHEE for routing manufacturing problems. Wu [45] developed a 4-D autonomous routing system for civil drone using a multi-step algorithm together with MACBETH. In the same lines, Jaishankar and Pralhad [46] develops an autonomous routing system for drone based on MCDA integration with GIS coupled with a distance transform technique. A combination of AHP and TOPSIS was presented by Yilmaz and Aplak [47] as a solution method for assessing alternative routes for a VRP. Dedemen [48] used AHP with PROMETHEE and GIS for the route selection of overhead power lines. Saini and Kumar [49] used AHP with fuzzy TOPSIS selection of best and most reliable route and provide alternative actions for making a robust Mobile Ad-hoc network. Ferreira, Costa, Tereso and Oliveira [50] presented a multi MCDA method for route planning of targets performing waste collection for recycling, based on AHP, SMART and Value Fn. Bandyopadhyay and Chanda [51] together with Bandni and Matrayee [52] used the Tarantula mating based multi-agent routing strategy together with PROMETHEE for routing manufacturing problems.

Ant colony algorithms are only just recently been utilized for swarm optimization for the dynamic vehicle routing problem [31], [53], [54]. Simulation studies of collaborative drone swarm [55] as a multi-agent system shows the possibility of successfully developing intelligent swarm applications. Nevertheless, reveals that in principle, as the number of networked drone increases, the model fails and evasive parallel processing algorithms are proposed to solve this problem. Other simulation studies use swarm intelligence and evolutionary algorithm based approach [56] for cooperation strategies of drone in their detection of targets. Most importantly, in drone swarm autonomy, the NVIDIA chip set has seen use in the determination of optimal routes for drone under varying wind conditions using the travelling salesman problem (TSP) algorithm [57], [58]. In another instance, this SoC has been used with generic ant colony optimization techniques to solve the TSP [20]. However, as the number of drone and the number of targets increase in a swarm, the algorithmic approaches used would need to rely in ever more efficient parallel processing techniques to achieve real-time detection.

The NVIDIA SoC is also used as a holistic middle ware for Adaptive Data processing and dissemination for Drone swarms in urban SENsing (ADDSEN) [59], indicating swarming with a partially ordered knowledge sharing distribution management system in a Wi-Fi network. The prototype system is based on the DJI Matrice 100 (M100) airframe with a Kinect "Guidance" system, the "Manifold" comprising the NVIDIA SoC; interfaced with a gimbal stabilized camera and an Arduino controller, which further interfaces the Wi-Fi module, sound, CO2, and PM sensors. On the other hand, MIT is already developing incredibly advanced autonomous drones that can navigate complex terrain and avoid obstacles at over 30 mph [60].

The SoC is also widely used in drone autonomy. When combined with a Robot Operating System (ROS) [61], a compliant flight control unit (FCU), which also contain sensor and actuator board [62] and being fully programmable, it provides the platform to accelerate development for autonomous capabilities of drone with novel autopilot algorithms. It is observed that ROS provides state of the art performance, at the fraction of respective embedded systems costs, with extensive scalability and flexibility in FCU and SoC choice and their respective sensors from a wide supplier base. Some of the benefits include:

1. HW abstraction - (works on NVIDIA, INTEL, QUALCOMM and AMBARELLA …)
2. FCU sensors - (magnetometer, accelerometer, gyroscope, barometer, sonar . . .)
3. SoC sensors / USB interface - (GPS, cameras, laser scanners . . .)
4. FCU / SoC communication - (simulation, testing, debugging)
5. SoC development - (acts as development machine as well as for in-flight controls)
6. Code compiles directly on FCU - (little downtime and no flashing)

An example of an autonomous take-off and landing system is developed using a visual based landing bay system for drone [63] which allows drone to extend their flight endurance, by enabling them to look for recharging stations, irrespective of the changes of the bay scene's illumination / shadows for viewing. Exploiting further the capabilities of the SoC, using the high frequency pose estimation of a known marker (thus eliminating transmission of the video stream off board) [64], with a frame rate of 30 fps and image resolution of 640x480 pixels. A similar system [65], but in which it relies on the pose estimate provided by the "Yellowstone" tablet from the Google's Tango project, demonstrates the prototype capabilities of the SoC as an autonomous flyer photographer. In case of drone system failure, a fault tolerant system [66] uses two heterogeneous hardware and software platform with

high assurance (HA) and high performance (HP) reliability platforms. During normal operation HP controls the drone. However, if it fails due to transient hardware faults or software bugs, the HA platform takes over, until the HP platform recovers. On the user interface capabilities, for a single operator to command and control a swarm of drones [67], the Naval Postgraduate School, has succeeded in launching 50 drone [68], apparently, a Guinness World Record for the number of drones under single operator control. Communication between drones was achieved via Wi-Fi using search and rescue operations algorithms. Being wing type Unmanned Aerial Vehicles (drone), launching them simultaneously posed some problems, limiting pre-flight launches to one every 30 seconds. On the other hand, requiring special approval from Federal Aviation Authority (FAA), INTEL [69] broke the previous world record coming up with a program that allowed the synchronized movements and light from 100 drones. Prenav [70] nowadays, develops drone that can fly closely to all structures, like cell towers and wind turbines. Prodrone drones even collects hazardous materials using robotic arms [71].

In our case study, we are dealing with high altitude UAV type MQ-1 Predator and considered their level of autonomy. The new system on chips, computer vision and open source code available on quadcopter UAV, considers future implementation to achieving full or cognitive autonomy on any UAV. We are more concerned about a routing system for a swarm of UAVs. From the current VRP taxonomies that exist, we identified that we are dealing with dynamic and deterministic vehicle routing problem. Recent algorithms in moving target VRP, genetic algorithms and ant colony optimization methods provide the platform for routing a swarm of UAVs to observe a swarm of MVs. Objective optimization methods, are intensely computer intensive and cannot be used in real time investigation, even with today's technology. As an alternative to optimization methods we study MCDA methodologies and observe how they have been also used for routing purposes. There are many MCDA techniques and integrating these techniques provide added advantages not possible as single MCDA method. Our paper defines for the first time in the literature a time-dependent multiple MCDA algorithm which ultimately provides routing autonomy, especially a swarm routing one. This is simply achieved by considering the investigation technique whether we inspecting and forgetting target suspiciousness, or inspecting without forgetting target suspiciousness, as it may become suspicious again in a later time. The different investigation techniques are described in Section 4.8.

3. Methodology

3.1 General overview

For our case study, we consider a set K of n suspect Maritime Vehicles MVk and a set S of m Unmanned Airborne Vehicles UAVj. The suspiciousness pk of each MVk is evaluated on ν criteria ci. As the criteria may depend on the initial location of the UAVj, the urgency of the intervention on an MVk is different for each UAVj and therefore, the priority ranking of the MVk will be different for each UAVj. Furthermore, the ranking will change after each single intervention as the environment is highly dynamic and thus a sequential and iterative decision-making process is adopted. Figure 2 shows a schematic overview of the decision support system, including the methods used, their data exchanges and interfaces.

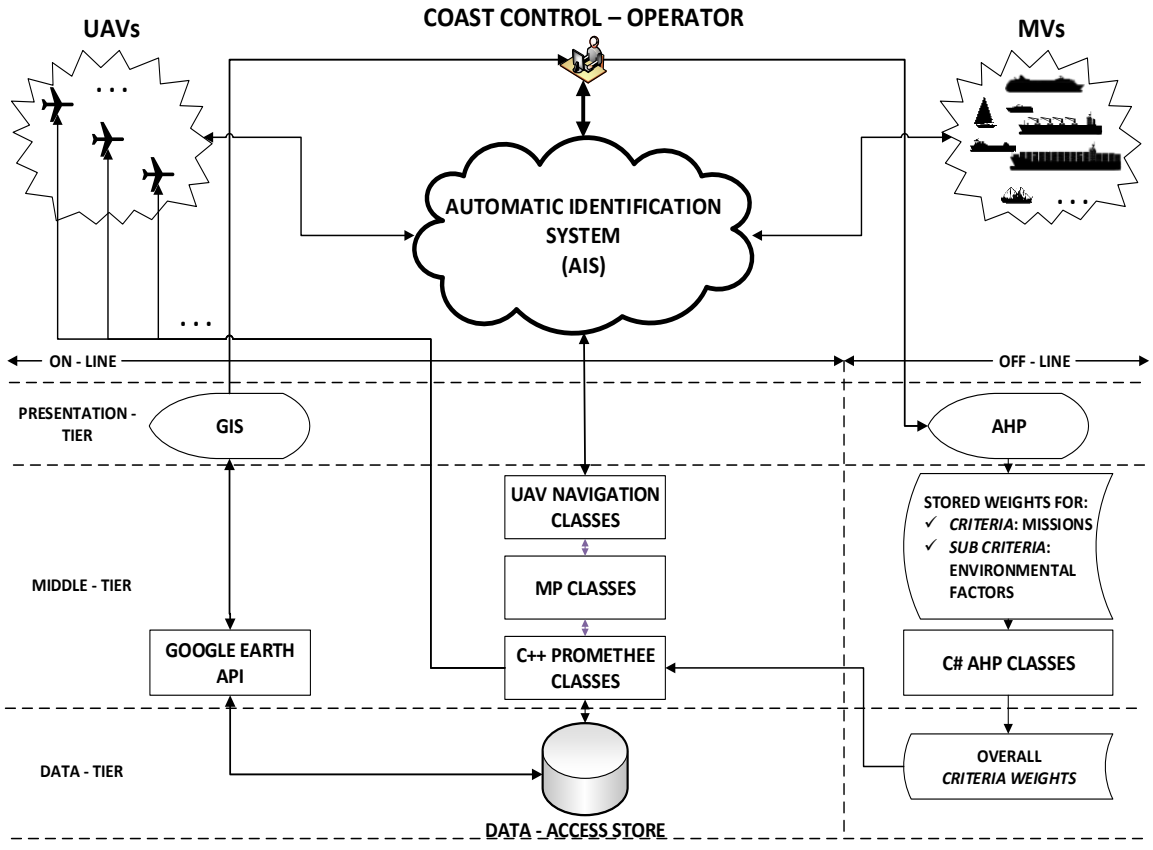

Figure 2: General overview of the decision support system (arrows indicate data flow)

The decision support system is to be integrated with the automatic identification system as used by operators in the coast ground control. It is developed on a three-tier architecture to encourage reusability, easy documentation and structured analysis. In addition, it allows the overall system to respond to changes, as when one tier is either improved or altered, the other tiers remain unaffected. The presentation-tier contains the graphical user interface and includes the functions that manage the interaction between the operator and the middle-tier. The middle-tier receives requests from the presentation-tier and returns results back to the presentation-tier according to the processing algorithms it contains. The middle-tier also calls the data-tier for information. The data-tier is responsible for storing the application data and sending it to the middle-tier as required.

3.2 Proposed multi MCDA

The stages of the developed MCDA decision support system in relation to each of the methods and their respective input(s) and output(s) are briefly summarized in Table 3. It is noted that the AHP methodology is an off-line process, meaning that all criteria weights calculations are predetermined. PROMETHEE, MP and GIS are online processes. The next sections describe all four stages in more detail.

Table 3. Processing stages of the developed decision support system at a particular decision-making sequence in time; arrows indicate data flow

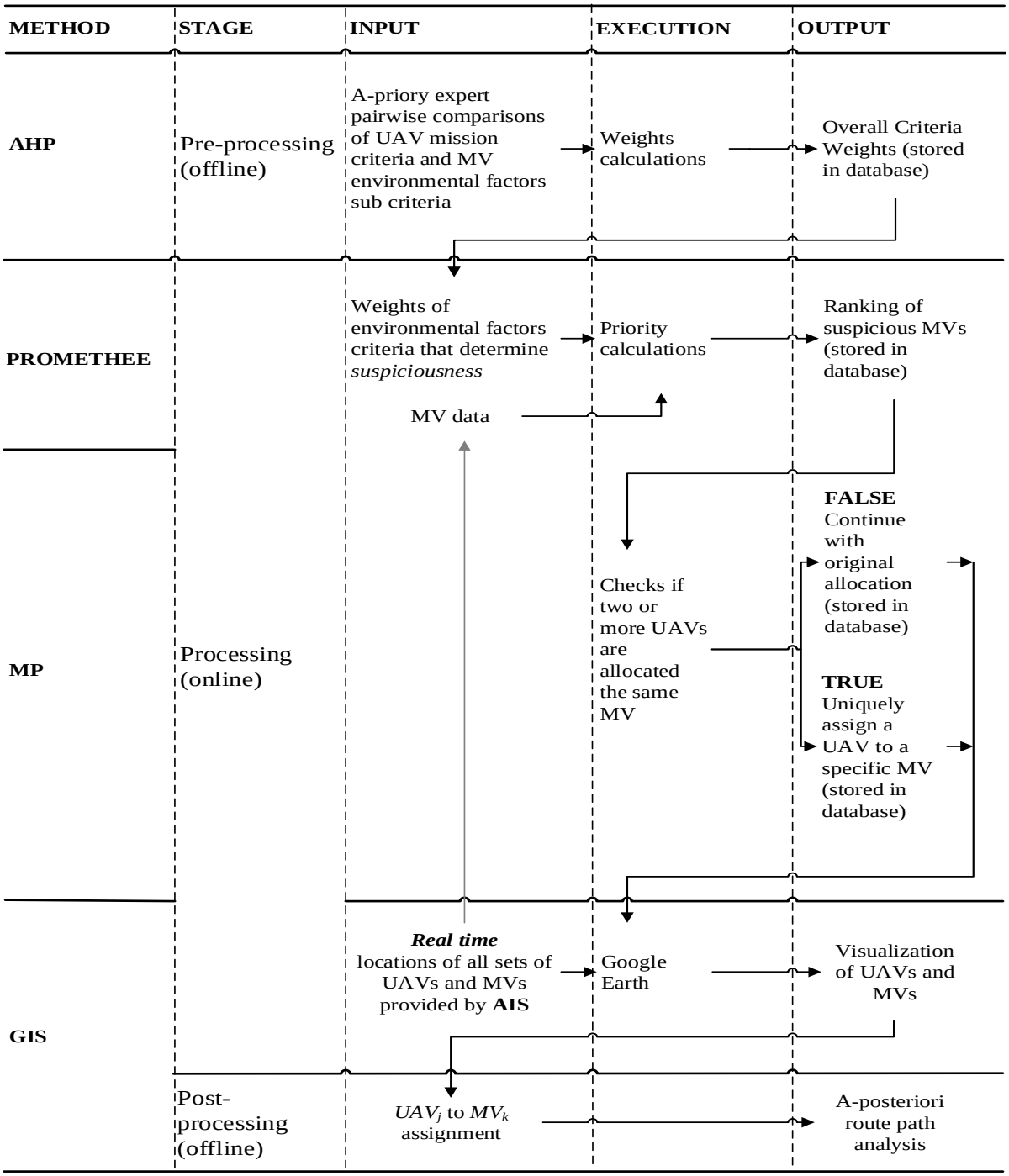

3.3 AHP: Weighting of suspiciousness criteria for MVs

The first stage focuses on structuring the problem with the definition of the UAV mission criteria and MV target factors sub criteria, as used to measure the suspiciousness of MVs. In this exercise, it is necessary to elicit the acquired knowledge of experienced human UAV operators, for example in a focus group. Once the problem is structured, the pairwise

comparison of the importance of each criterion is evaluated in a comparison matrix A. Weights are calculated with Saaty's [72]–[74] eigenvalue method of AHP:

$$A \cdot p = \lambda_{max} \cdot p \quad (1)$$

where, A is the comparison matrix

p is the priority (weight) vector

λ_{max} is the maximal eigenvalue

A consistency of the evaluations can be measured with the consistency index (CI):

$$\mathrm{CI} = \frac{\lambda_{max} - n}{n - 1} \quad (2)$$

where, n is the dimension of the matrix

λ_{max} is the maximal eigenvalue

If the consistency ratio of the consistency and the random indexes is less than 10%, then the matrix can be considered as having an acceptable consistency [75].

3.4 PROMETHEE: Ranking of suspicious MVs

In the second stage, the suspiciousness of the maritime vehicles is ranked using PROMETHEE [76]. This method has been adopted mainly because once its parameters are defined, it can be fully automated. It also has a very low computing time, which is essential in a dynamic environment for real-time calculations. PROMETHEE is an outranking method, a compromise between the too poor dominance relations and the excessive ones generated by utility functions. This is important, as every outranking method includes two phases:

- Construction of an outranking relation,
- Exploitation of this relation to assist the decision-maker.

In our case study, it compares pairwise the suspiciousness of each maritime vehicle, by calculating the difference between the suspiciousness criteria evaluation of the two MVs on the criterion i:

$$d_i(MV_k, MV_f) = f_i(MV_k) - f_i(MV_f) \quad (3)$$

where, $d_i(MV_k, MV_f)$ is the difference between the evaluations of two alternatives (i.e. MVs) for one criterion f_i.

This difference is introduced in the preference function of criterion i, which gives the unicriterion preference degree. Several preference functions exists [76], Equation 4 depicts a linear preference function:

$$P_{kf}^{i} = \begin{cases} 0, & if\ d_i(MV_k, MV_f) \le q_i \\ \dfrac{d_i(MV_k, MV_f) - q_i}{p_i - q_i}, & if\ q_i < d_i(MV_k, MV_f) \le p_i \\ 1, & if\ d_i(MV_k, MV_f) > p_i \end{cases} \quad (4)$$

where, q_i is the indifference threshold

p_i is the preference threshold

If qi = pi, then we have a step function as shown in Figure 3.

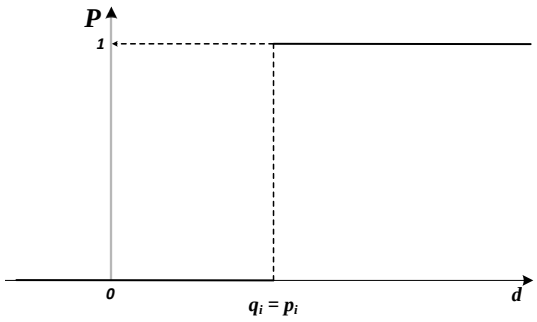

Figure 3: A step function

Anything equal or below the indifference point has a preference of 0, above it has a preference of 1. A preference degree of 1 means a total preference for one action on the considered criterion. A preference of 0 means that there is no preference at all. The indifference and preference threshold are the boundaries for these two extreme preferences.

The global preference degree is given by the weighted sum of the unicriterion preference degree:

$$\pi(MV_k, MV_f) = \sum_{i=1}^{n} P_{kf}^{i}(MV_k, MV_f) \cdot w_i \qquad (5)$$

where, w_i represents the weight of criterion ci.

To compare every maritime vehicle with respect to all the others, two scores are computed. The positive outranking flow (6) expresses how a maritime vehicle outranks all the others. It represents its power (outranking) character. The higher $\phi^{+}(MV_k)$ is, the more preferred the action is. The negative outranking flow (7) expresses how a maritime vehicle is outranked by all the others. The lower $\phi^{-}(MV_k)$ is, the worse the action is.

$$\phi^{+}(MV_k) = \frac{1}{n-1} \sum_{MV \in K} \pi(MV_k, MV) \qquad (6)$$

$$\phi^{-}(MV_k) = \frac{1}{n-1} \sum_{MV \in K} \pi(MV, MV_k) \quad (7)$$

Thence, the positive and negative preference flows are aggregated into the net preference flow:

$$\phi(MV_k) = \phi^{+}(MV_k) - \phi^{-}(MV_k) \quad (8)$$

The PROMETHEE ranking is obtained by ordering the alternatives (MVs) according to the decreasing values of the net flow scores. We note that it should also be possible to develop a weighting and scoring scheme for a Multi-Attribute Value Analysis (MAVA) approach as the criteria are all reduced and expressed in the same unit (in this case through value functions) which replicates most of what is done here via AHP and PROMETHEE.

3.5 MP: Multiple UAV allocation

In rare case of two or more UAVs having the same first allocated target, the tie is broken by modelling an assignment problem (25). The global objective function is to maximise the total suspiciousness of the MVs that will be investigated by the fleet of UAVs. If UAVj is sent to observe MVk, then x_{jk} is assigned 1 otherwise 0.

$$max \sum_{j \in S} \sum_{k \in K} p_{jk} \cdot x_{jk} \quad (9)$$

subject to:

$$\forall k \in K \ \sum_{j=1}^{m} x_{jk} \leq 1 \ \left[for\ each\ MV_k\ at\ most\ one\ UAV_j\ is\ allocated\right]$$

$$\forall j \in S \quad \sum_{k=1}^{n} x_{jk} \leq 1 \ \left[for\ each\ UAV_j\ at\ most\ one\ MV_k\ is\ assigned\right]$$

$$x_{jk} \in (0,1), \qquad \forall j \in S, \qquad \forall k \in K$$

where, p_{jk} is the suspiciousness value calculated by PROMETHEE.

After a MV has been fully investigated, it is removed from the list of suspect MVs, while the criteria characteristics of the remaining (unvisited) MVs are updated. PROMETHEE is used again to calculate a ranking for the next assignment.

3.6 GIS: Visualization

A Geographic Information System (GIS) allows to visualise, question, analyse, and interpret data on a geographical map to understand relationships, patterns, and trends [77]. GIS allows the collection of data which can be overlain on the base map to create geo-referenced renderings. It is a tool that links features on a map with data. The linking of map features and data is commonly known as 'spatial data' and it proved to be useful when integrated with AHP and PROMETHEE methodologies [78]–[81]. Distinct map layers for each UAV and MV, are created and then by overlaid on Google Earth to visualize the whole scenario of amphitheatre, collectively in real time. Each layer consists of spatial data describing the route path of each MV and the calculated routing path of each UAV. As this information is stored in the database, the GIS module implemented should improve a posteriori decision-making by enabling supplementary analysis of the data.

3.6.1 UAV Navigation

Each MV and UAV is tabulated in a file, based on the guidelines of the Earth Point site [82]. Then, each file is converted to a Keyhole Mark-up Language (KML) file, using the Earth Point tools provided. This allows to simulate the sequential MV allocation problem to utilize Google Earth as a visualization tool.

In every interval time and for each MVk, the AIS provides their initial geographic coordinates ($lat_{MV_k}(t), lon_{MV_k}(t)$) in radians, as well as their initial bearing in degrees, $BRG_{MV_k}(t)$, at time, t (i.e. current time). Based on this information, the location of each MVk, ($lat_{MV_k}(t'), lon_{MV_k}(t')$) and bearing travelling along a (shortest distance) great circle arc $BRG_{MV_k}(t')$ for the next time interval t', are calculated. Thence, once the rankings BRG of MVs suspiciousness scores are obtained, a UAV is instructed to change its direction (route) and lock to the MV with the highest ranking (i.e. being most suspicious). In other words, we wish to navigate an UAV at time t, to the location of the most suspicious MV with actual coordinates ($lat_{MV_k}(t'),\ lon_{MV_k}(t')$) as bearing. It is to note that the change of velocity in the interval t – t' is possible and cannot be predicted. MV speed calculations are shown in Appendix 7.1.

Similarly to MVs, at initial time, t, for each UAV (as shown in Figure 4) their position can be defined by ($lat_{UAV}(t), lon_{UAV}(t)$) which is the initial starting point (latitude, longitude) of the UAV in radians and $BRG_{UAV}(t)$ which is the initial bearing of the UAV in radians, clockwise from North. The destination point of the UAV, ($lat_{UAV}(t'),\ lon_{UAV}(t')$) and final predicted heading travelling along a (shortest distance) great circle arc ($HDG_{UAV}(t')$) in the next time interval, t', towards the most suspicious MV, is calculated using the Movable Type Scripts [83]. In other words, the UAV heading calculations are done in the previous time interval, after the MV bearing calculations are completed. Simply the UAV is steered where the MV was with time steps that are small enough that the sensor angle will accommodate any difference. Moreover, UAVs generally travel faster than MVs, so that the error is not large. For simplicity t – t' is constant at UAV velocity of 140 km h-1. In each case, we calculate the distance of the UAV to the MV at time t and then only proceed with predicting the future, t', locations and adjustments if that distance is larger than the maximum camera range (10 km). This may be true for larger UAVs and large ships, but for smaller drones reacting to small agile MVs – such as speed-boats – the errors could be more significant.

$$lat_{UAV}(t') = \text{asin}(\sin(lat_{UAV}(t\ \ )) \times \cos\left(\frac{d}{ER}\right) + \cos(lat_{UAV}(t\ \ )) \times \sin\left(\frac{d}{ER}\right) \times \cos(BRG_{UAV}(t\ \ )) \quad (10)$$

where, d is the distance travelled by a UAV per time interval (constant).

ER is the Earth's Radius (6371 km) d / ER is the angular distance (radians)

$$lon_{UAV}(t') = lon_{UAV}(t\ \ ) + atan2(w, x) \quad (11)$$

where,

$$w = \cos\left(\frac{d}{ER}\right) - \sin(lat_{UAV}(t')) \times \sin(lat_{UAV}(t\ \ )) \quad (12)$$

$$x = sin(BRG_{UAV}(t_0)) \times sin\left(\frac{d}{ER}\right) \times cos(lat_{UAV}(t\ \ )) \quad (13)$$

The new UAV heading is calculated by:

$$HDG_{UAV}(t') = atan2(y, z) \quad (14)$$

where,

$$y = \cos(lat_{UAV}(t')) \times \sin(lat_{MV_\kappa}(t')) - \sin(lat_{UAV}(t')) \times \cos(lat_{MV_\kappa}(t')) \times \cos(lon_{MV_\kappa}(t') - lon_{UAV}(t')) \quad (15)$$

$$z = \sin\left(lon_{MV_\kappa}(t') - lon_{UAV}(t')\right) \times \cos(lat_{MV_\kappa}(t')) \quad (16)$$

Thereafter, the process is repeated for each interval of time to route the UAV to the most suspicious MV.

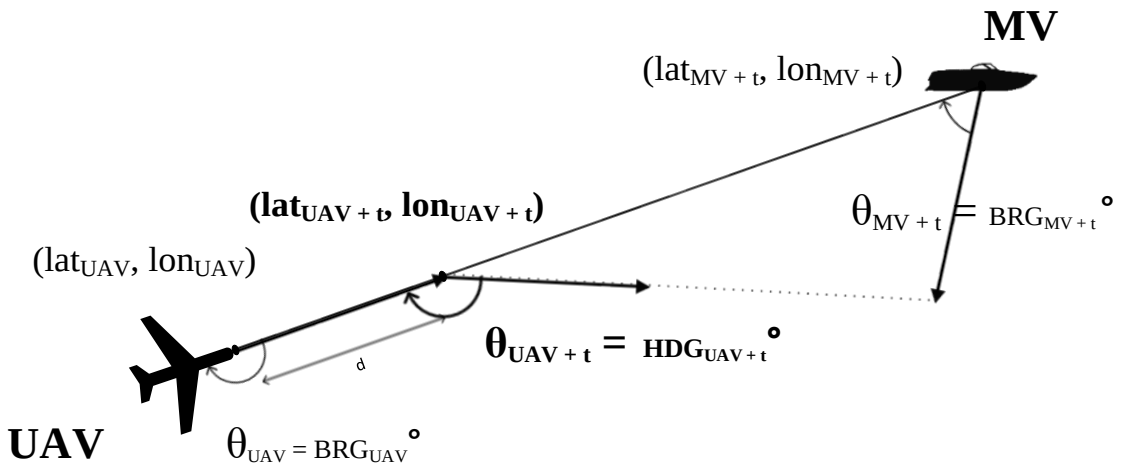

Figure 4 Plan view of UAV navigation

Finally, the distance of the UAV to the most suspicious MV, $Dist_{UAV-MV}$ is determined (to allow making the decision when to terminate the investigation) by the spherical laws of cosines (at sea level):

$$\begin{aligned} Dist_{UAV-MV} = \text{acos}(&\sin\left(lat_{UAV}(t')\right) \times sin\left(lat_{MV_\kappa}(t')\right) \\ &+ \cos \times lat_{UAV}(t') \times \cos\left(lat_{MV_\kappa}(t')\right) \times \cos(lon_{MV_\kappa}(t') \\ &- lon_{UAV}(t'))) \times ER \end{aligned} \quad (17)$$

For simplification, we consider UAVs to be type MQ-1 Predator, which has a max speed of 309 km/hr and can reach altitudes of 30,000 ft. The UAVs in our case study is flying at a fixed height, h (7.6 km – 25,000 ft), from the sea level, and thus use Pythagoras's theorem of

equirectangular projection which suffices to calculate the actual distance, D_A of the UAVj to the most suspicious MVk (Figure 5).

$$D_A = \sqrt{Dist_{UAV-MV_\kappa}{}^2 + h^2} \tag{18}$$

As an assumption, the UAVs will stay locked to the MV until the distance between them is less than or equal to the maximum camera range, which is the maximum range that a UAV can investigate (i.e. photograph) the suspicious MV.

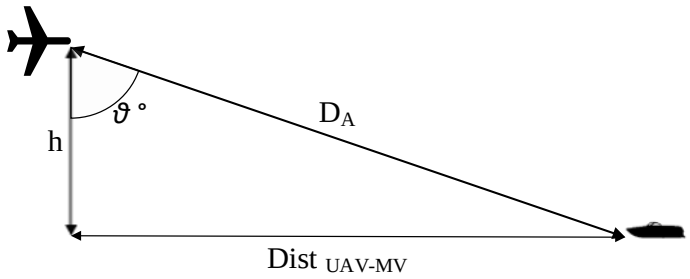

Figure 5 Actual distance

If this condition is satisfied (UAV completes the investigation of the MV), then the specific MV is removed from the list of UAVs to investigate and a new PROMETHEE ranking is re-calculated to define the next MV to investigate. This procedure is repeated, until all MVs are investigated.

3.6.2 Area Criteria Algorithm

The varying MV parameters related to the position of the MV, as provided by the aviation experts from Alenia Aermacchi [84], include:

Latitude (radians)

Longitude (radians)

Bearing (radians)

These parameters are used to calculate the distance of the UAV to coast, and the distance of UAV to island. However, the distance is not used as a row data in the criteria as the suspiciousness is not simply inversely linearly correlated to the distance. An Area Criteria Algorithm based on the sigmoid function (or logistic function) is used:

$$\mathrm{CRIT}_{\mathrm{Area}}\left(\mathrm{lat}_{MV_\kappa}, lon_{MV_\kappa}, \mathrm{HDG}\right) = \mathrm{CRIT}_{\mathrm{Angle}}(\mathrm{lat}_{\mathrm{AOI}}, \mathrm{lon}_{\mathrm{AOI}}, \mathrm{HDG}) \times \mathrm{CRIT}_{\mathrm{Range}}(\mathrm{lat}_{AOI}, \mathrm{lon}_{\mathrm{AOI}}) \quad (19)$$

where, $(\mathrm{lat}_{MV_\kappa}, lon_{MV_\kappa})$: are the given geographical coordinates in radians (latitude, longitude) of the MV.

HDG: is the MV heading at given instance of time.

$(\mathrm{lat}_{AOI}, \mathrm{lon}_{\mathrm{AOI}})$: is the fixed geographical coordinates in radians (latitude, longitude) at the centre of area of interest (AOI), i.e. island or coast

The angle criteria, $\mathrm{CRIT}_{\mathrm{Angle}}$ is given by,

$$\mathrm{CRIT}_{\mathrm{Angle}}(\mathrm{lat}_{\mathrm{AOI}}, \mathrm{lon}_{\mathrm{AOI}}, \mathrm{BRG}) = \frac{1 + \mathrm{e}^{-\beta_a \times (1 - \cos(\alpha))}}{1 + \mathrm{e}^{(-\beta_a \times (\cos(\mathrm{BRNG} - \mathrm{HDG}) - \cos(\alpha))}} \quad (20)$$

where, α: is the limiting angle, asymptote of the sigmoid function.

β_a: is the steepness of the sigmoid for the angles/heading criteria

The denominator is used to normalize the function, whereas the bearing (BRG) is given by:

$$\mathrm{BRG} = \operatorname{atan2}(\sin(\mathrm{lon}_{\mathrm{AOI}-}\mathrm{lon}_{MV_\kappa}) * \cos(lat_{AOI}), \cos(lat_{MV}) * \sin(lat_{AOI}) - \sin(lat_{AOI}) * \cos(lon_{\mathrm{AOI}-} lon_{MV_\kappa}) \quad (21)$$

The range criteria is given by,

$$\mathrm{CRIT}_{\mathrm{Range}}(\mathrm{lat}_{AOI}, \mathrm{lon}_{AOI}) = \frac{1 + \mathrm{e}^{-\beta_r}}{1 + \mathrm{e}^{-\beta_r \times (\frac{\mathrm{dist}}{\mathrm{range}} - 1)}} \quad (22)$$

where, β_r: is the steepness of the sigmoid for the range criteria

range: is a dimensional unit, which expresses the urgency of an MV as a distance from the centre of an AOI (asymptote of sigmoid function).

dist: the distance given by:

$$\mathrm{d} = \mathrm{ER} \times \mathrm{c} \quad (23)$$

where, ER (Earth's Radius) = 6371 km

$$\mathrm{c} = 2 * \operatorname{atan2}(\sqrt{\mathrm{a}}, \sqrt{1 - \mathrm{a}}) \quad (Haversine\ formula) \quad (24)$$

where,

$$\mathrm{a} = \sin^2((\mathrm{lat}_{AOI} - \mathrm{lat}_{MV_\kappa})/2) + \cos(lat_{AOI}) * \cos(\mathrm{lat}_{MV_\kappa}) * \sin^2((\mathrm{lon}_{AOI} - \mathrm{lon}_{MV_\kappa})/2) \quad (25)$$

4. Case Study

4.1 Introduction

UAVs used in our case study with 15 MVs is illustrated. Figure 6 shows their initial location and their arrow indicates their direction. MV1, MV2, MV3 and MV4 are considered suspicious in the context of drug trafficking. Specifically, MV1, MV2, MV3 are small speed boats initially starting from the shores of Sicily. They all meet with MV4, a large cargo ship travelling parallel to the shore of Sicily and approximately 70 kilometres from the coast; which also detours slightly inwards to the coast to meet with the speed boats. The speed boats meet the cargo ship consecutively. After a so-called rendezvous (agreed meeting location), all speed boats return to the shores of Sicily and the cargo ship resumes original bearing as before detouring. The remaining marine vehicles MV5 – MV15 are considered suspicious for illegal immigration.

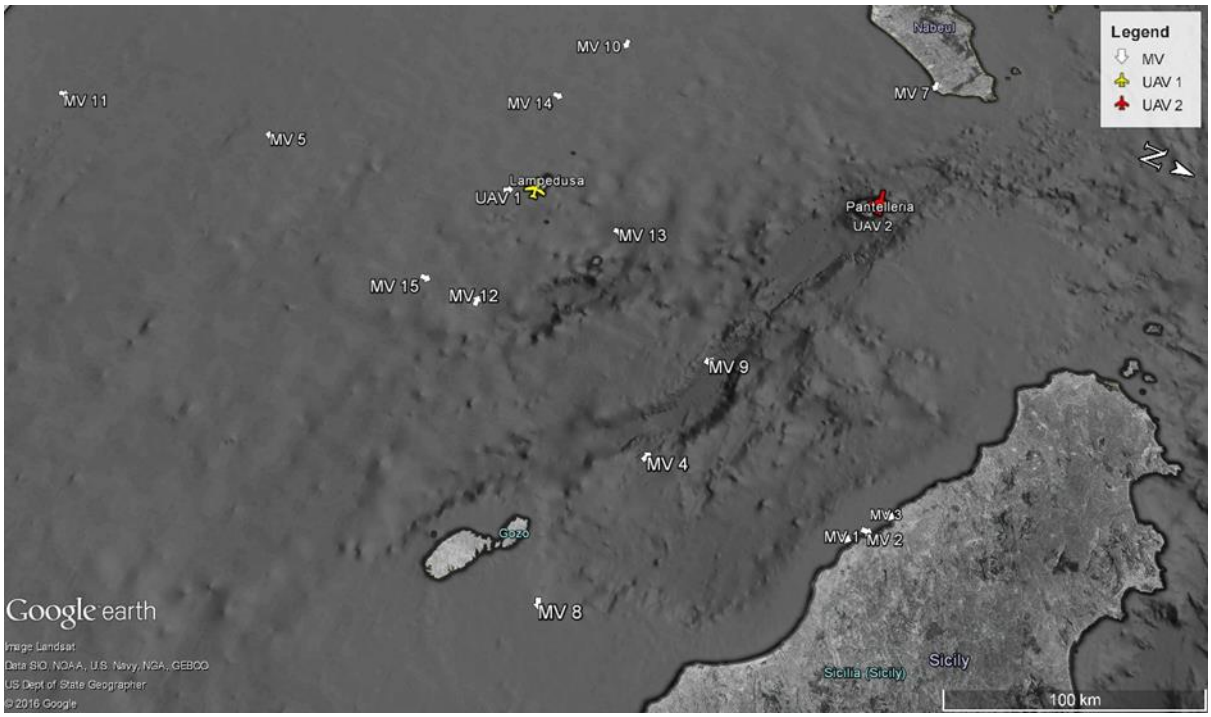

Figure 6: Google Earth simulation for 2 UAVs and 15 MVs at initial time: 16:30

Two UAVs are chosen to implement the surveillance of the fifteen suspicious MVs. At 16:30, UAV1 takes off from Lampedusa, and simultaneously UAV2 takes off from Pantelleria. Figure 6 shows the locations of the two UAVs and the 15 MVs at initial time 16:30. The

simulation is run in intervals of 5 minutes, until 21:15 and is described further in Section 4.6. In the next section, UAV mission criteria and MV target sub criteria are determined.

4.2 AHP: Hierarchy Design

The criteria were elicited in a focus group of human UAV operators and mission planners. However, we were not invited in the elicitation of the knowledge as this was a defence classified exercise. We only know that it was elicited in a focus group. On a post-discussion, they were very confident with the list of criteria. It is also noted that it would be very easy to add or remove criteria from the model if required. Four mission criteria have been considered for the theatre of the operations. These include:

1. Drug trafficking near the island (Lampedusa)
2. Drug trafficking near the coast (Marina di Palma)
3. Illegal immigration during the day
4. Illegal immigration during the night

The missions are evolving and not mutually exclusive. For example, drug trafficking and illegal immigration can happen at the same time. For each UAV mission, the definition of suspiciousness is determined by both UAV mission criteria as well as MV target sub criteria. These include:

C1: Dimension of the MV [m]: small MVs are more difficult to detect than large MVs.

C2: Change of speed [km/h]: large increases or decreases of MV's speed for no reason increases suspiciousness. For example, a decrease in the speed of MVs could mean that they could be slowing down to approach each other, whereas sudden increase of the speed of small MVs makes them ultimately more suspicious for both drug trafficking or illegal immigration.

C3: Rendezvous [km]: A small distance between MVs could indicate a meeting, probably to exchange illicit goods. The distance between the MV and its closest neighbour is recorded.

C4: Distance to island [km]: The closer to the island (e.g. Lampedusa in mission a), the more urgent an investigation is, which may indicate illegal immigration.

C5: Distance to coast [km]: The closer to the coast (e.g. Marina di Palma in mission b), the more urgent an investigation is, which may indicate drug trafficking.

C6: Distance UAV to MV [km]: The shorter the 'travel time' will be. Hence, the faster a UAV can reach at the MV of interest.

C7: MAOC tagging [binary criterion (0 = false; 1 = true)]: the operator in Maritime Analysis and Operations Centre (MAOC) has information to indicate that the MV is highly suspicious and recommend an urgent investigation.

The distances Being close to island (C4) and Being close to coast (C5) are further processed with the Area Criteria Algorithm (ACA) to define the urgency (Section 3.6.2). These criteria have output values between 0 and 1, where 1 indicates an extreme urgency and 0 means that it is not urgent. The Change of speed (C2), Distance to island (C4), Distance to coast (C5), and the MAOC tagging (C7) criteria are to be maximized in PROMETHEE. The remaining criteria are to be minimised. In the Appendix 7.1, it can be seen how the criteria are calculated. The structure (scenario) of the problem (Figure 7) has four levels. The main goal is to define the suspiciousness of MVs. The second level contains the criteria, which are the set of missions that UAV are going to tackle. The third level is composed by the sub-criteria describing the MV. Finally, the MV are the on the last level. Each element relates to all the elements of their immediate upper and lower level. For readability reasons, not all connections have been drawn on Figure 7.

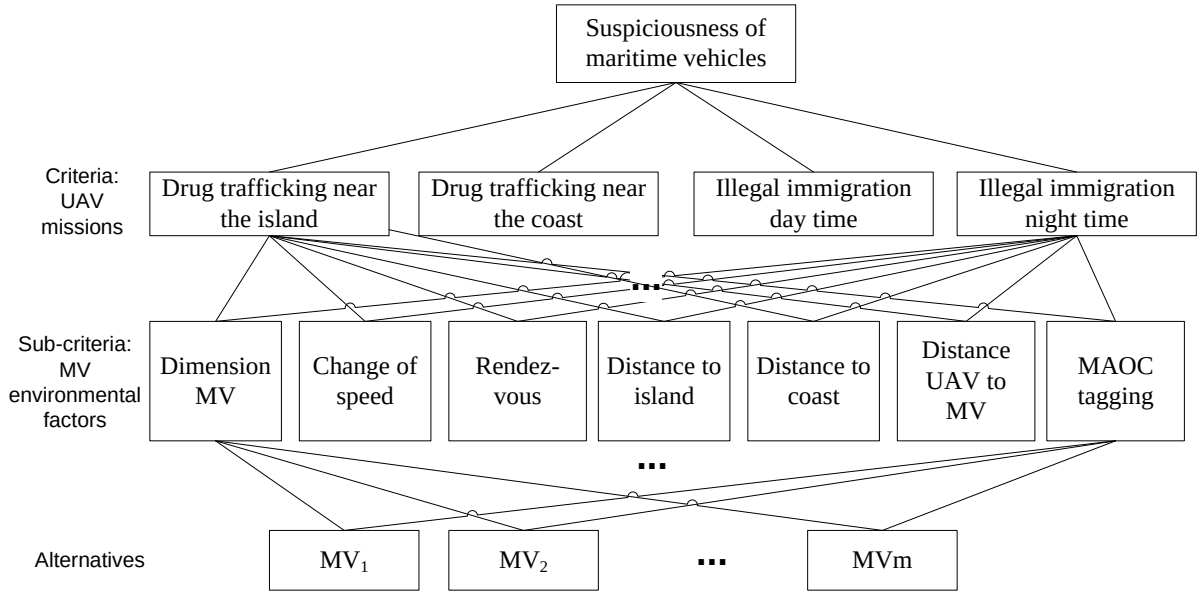

Figure 7: Hierarchy defining the criteria and sub criteria

4.3 AHP: Mission criteria weighting

Although the mission starts for both UAV1 and UAV2 simultaneously, due to their different geographical location, the scenario is thus different for each UAV. UAV1 is more concerned with illegal immigration, whilst UAV2 is more dedicated to drug trafficking. By consequence, their scenario weights are different. The most appropriate scenario is evaluated by the experts using pairwise comparisons in Figure 8 for UAV1 and in Figure 9 for UAV2. Note, "Drug trafficking sea" and "Drug trafficking near the island" apparently is being used to describe the same MV activity. In our Decision Support System (DSS) a customised AHP software has been developed in C# to automatically feed the weights into PROMETHEE; which is not possible with an independent commercial software package. The Graphical User Interface (GUI) is shown in Figure 8 and Figure 9. The scenario priorities are given in Table 4. Our AHP software evaluates an overall set of missions (see first level in Figure 7) that UAVs can address.

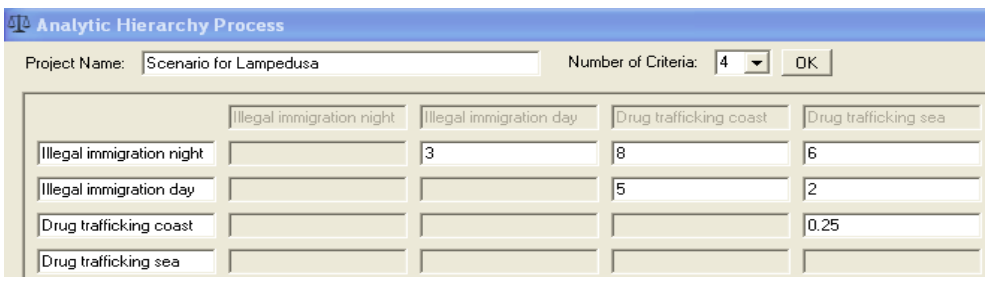

Figure 8: Pairwise comparisons of the scenario for UAV_1

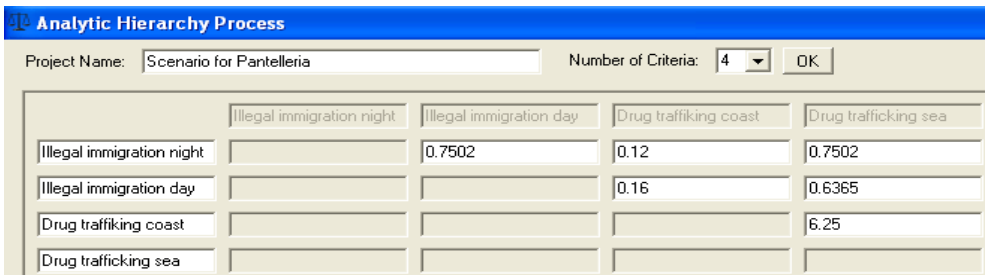

Figure 9: Pairwise comparisons of the scenario for UAV_2

Table 4: Mission priorities for each UAV scenarios

Priorities	***UAV₁***	***UAV₂***
Drug trafficking near the island	0.1307	0.1249
Drug trafficking near the coast	0.0488	0.6925
Illegal immigration during the day	0.2259	0.0995
Illegal immigration during the night	0.5946	0.0831
Consistency ratio	0.043	0.0001

4.4 AHP: Target criteria weighting

The criteria defined in section 0, are prioritised using pairwise comparisons by the sea border surveillance experts for all missions (Figure 10). The calculated weights are given in Table 5.

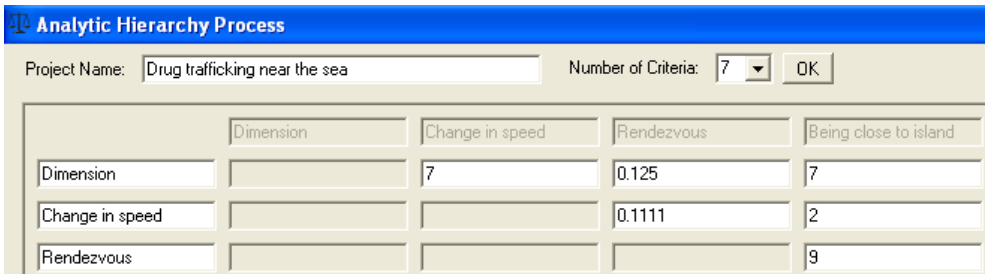

Figure 10: Pairwise comparison of the target criteria for the drug trafficking near the coast mission

All comparison matrices are consistent (i.e. CR ≤ 10 %). The MAOC tagging is the most weighted criterion. This result was expected as the MAOC is based on the possession of

external information indicating a particularly high suspicious MV. In our case study, all MVs are tagged. The distance to coast is highly important in the scenario "Drug trafficking near the coast". In the other scenarios, the coast may be far away, and therefore this criterion is less important. As a rendezvous in the middle of the sea is highly improbable because MVs tend not to be close to each other to avoid collisions, this behaviour is highly suspicious. A change of speed in the night is unlikely because of security reasons. Therefore, it has a higher weight in the night scenario. The distance UAV to MV obtains generally a low weight because UAVs are much faster than MVs.

Table 5: Target criteria weights for different mission criteria

Criteria	**Drug coast**	**Drug sea**	**Immigration day**	**Immigration night**
Dimension	0.108	0.103	0.092	0.165
Change of Speed	0.039	0.023	0.031	0.144
Rendezvous	0.040	0.321	0.025	0.020
Distance to island	0.034	0.020	0.155	0.063
Distance to coast	0.319	0.033	0.150	0.221
Distance UAV to MV	0.034	0.166	0.030	0.083
MAOC tagging	0.426	0.334	0.518	0.304
Consistency Ratio (CR)	0.06	0.09	0.07	0.09

4.5 AHP: Suspiciousness criteria weighting

As the UAVs are operating with different mission criteria, target sub-criteria (Table 5) need to be multiplied by the mission criteria (Table 4) of the respective UAV. The final suspiciousness criteria weights for each UAV are shown in Table 6

Table 6: The final suspiciousness criteria weights for each UAV

	Criteria	UAV_1	UAV_2
C_1	Dimension	0.139	0.111
C_2	Change of Speed	0.104	0.047
C_3	Rendezvous	0.062	0.079
C_4	Distance to island	0.069	0.044
C_5	Distance to coast	0.184	0.252
C_6	Distance UAV to MV	0.084	0.059
C_7	MAOC tagging	0.358	0.408

The suspiciousness criteria weights for UAV1 and UAV2 (Table 6) are used to dynamically rank MVs using PROMETHEE as is described in the next section.

4.6 PROMETHEE: Dynamic MV ranking

Fifteen MVs are to be investigated. For each MV, their location, heading and speed are transmitted to the decision support system by the automated identification system or if absent by fixed land radars and satellites. The sub criteria dimension (C1) is independent of time and the considered UAV. Change of speed (C2), rendezvous (C3), distance to island (C4), distance to coast (C5) and to some extent the MAOC (C7) tagging are time-dependent but independent from the observing UAV. The Distance UAV to MV (C6) is dependent on time and the observing UAV. Scores of the first allocation (16:30) for UAV1 are given in Table 7 and are calculated with the formula given in Appendix 0. Scores of a second allocation (16:45) for UAV1 are given in Table 8. The weights of the criteria are provided from Table 6. The choice of values for preference and indifference thresholds were chosen by the experts on their presumptions of reasonable boundaries.

Table 7: Tables of scores on the first Allocation to UAV_1 at time 16:30

	C_1	C_2	C_3	C_4	C_5	C_6	C_7	
Min/Max	**MIN**	**MAX**	**MIN**	**MAX**	**MAX**	**MIN**	**MAX**	
Pref. fn	Linear	Linear	Linear	Linear	Linear	Linear	Linear	
Preference	20	0.001	20	1	1	40	1	
Indifference	8	0	2	0	0	10	0	
Inflection	n/a	n/a	n/a	n/a	n/a	n/a	n/a	
Weight	**0.139**	**0.104**	**0.062**	**0.069**	**0.184**	**0.084**	**0.358**	***MV Ranking***
MV 1	12	0	9.043	0.691	0.685	207.041	1	0.008
MV 2	8	0	9.043	0.973	0.551	210.297	1	0.023
MV 3	20	0	11.64	0.985	0.908	212.091	1	0.122
MV 4	60	0	46.416	0.919	0.843	135.964	1	-0.236
MV 5	12	0	108.862	0.805	0.914	131.736	1	0.017
MV 6	**8**	**0**	**55.751**	**0.707**	**0.941**	**12.785**	**1**	**0.323**
MV 7	20	0	151.582	0.704	0.577	201.144	1	-0.329
MV 8	60	0	78.064	0.661	0.768	188.331	1	-0.485
MV 9	12	0	46.416	0.675	0.818	114.486	1	0.082
MV 10	8	0	46.231	0.977	0.95	95.321	1	0.260
MV 11	20	0	108.862	0.974	0.729	240.577	1	-0.251
MV 12	60	0	25.359	0.959	0.819	61.459	1	-0.032

MV 13	12	0	55.751	0.728	0.772	44.697	1	0.164
MV 14	8	0	46.231	0.66	0.806	53.966	1	0.214
MV 15	20	0	25.359	0.678	0.579	66.141	1	0.12

UAV_1 routes to investigate *MV_6* as it is the first (highest) ranked.

Table 8: Tables of scores on the second allocation to *UAV_1* at time 16:45

	C1	**C_2**	**C_3**	**C_4**	**C_5**	**C_6**	**C_7**	
Min/Max	**MIN**	**MAX**	**MIN**	**MAX**	**MAX**	**MIN**	**MAX**	
Pref. fn	Linear	Linear	Linear	Linear	Linear	Linear	Linear	
Preference	20	0.001	20	1	1	40	1	
Indifference	8	0	2	0	0	10	0	
Inflection	n/a	n/a	n/a	n/a	n/a	n/a	n/a	
Weight	**0.139**	**0.104**	**0.062**	**0.069**	**0.184**	**0.084**	**0.358**	***MV Ranking***
MV_1	12	0	9.043	0.691	0.685	197.567	1	-0.085
MV_2	8	0	9.043	0.973	0.551	201.404	1	-0.073
MV_3	20	0.037	11.01	0.977	0.578	195.009	1	0.073
MV_4	60	0.041	30.397	0.939	0.657	122.15	1	-0.129
MV_5	12	0	74.324	0.825	0.856	137.187	1	-0.072
MV_7	20	0	150.365	0.899	0.638	200.435	1	-0.361
MV_8	60	0	86.26	0.994	0.659	167.196	1	-0.554
MV_9	**12**	**0.045**	**30.397**	**0.663**	**0.829**	**95.352**	**1**	**0.324**
MV_{10}	8	0	36.624	0.975	0.699	101.887	1	0.059
MV_{11}	20	3.022	74.324	0.966	0.961	211.033	1	0.143
MV_{12}	60	0	26.623	0.949	0.821	37.293	1	-0.120
MV_{13}	12	0	47.851	0.728	0.77	43.98	1	0.086
MV_{14}	8	0	36.624	0.661	0.806	71.302	1	0.110
MV_{15}	20	0	26.623	0.678	0.579	52.574	1	0.024

At 16:45, UAV1 investigation of MV6 is completed and thus removed from the PROMETHEE rankings (Table 8). Also, the suspiciousness of remaining MVs have changed. The new ranking shows that MV9 is now most suspicious (e.g. it is now near to the island and its speed has increased), and thus it is the next MV to be investigated. When MV9 investigation is then completed, the table of scores is updated and a new PROMETHEE ranking is re-calculated. This procedure is also simultaneously repeated for UAV2 (taking off from Pantelleria). In the next section, the routing visualisation of UAV1 and UAV2 on the Google Earth GIS is presented.

4.7 MP: Multiple UAV allocation

In this case study, there are no ranking ties between any MVs by the two UAVs. Nevertheless, it is deemed that as the number of UAVs and MVs increases, the possibility of ranking ties could come into action, and the mathematical programming methodology for solving the assignment problem between two MVs with equal rank ties, as presented in section 3.4, would then facilitate in determining the most suspicious MV for each UAV. This step is important avoid errors as sending two UAV to the same target could have catastrophic consequences, if a vessel with abnormal behaviour has a navigation problem and is in danger to sink, then a delay in investigation would costs human lives.

4.8 GIS: Route visualization

Given the initial UAV coordinates and heading (i.e. take-off at the airport) and the coordinates and heading of the most suspicious MV, the sequential MV allocation is calculated with the methodology presented in Section 3.5. The order of MV investigation by the two UAVs is shown in Figure 11. The detailed calculations are in the in the supplementary materials. All tracking is done using Google Earth GIS as a visualization tool.

The swarm autonomous simulation for a multicriteria (inspec and forget) system, can be seen on:

https://www.youtube.com/watch?v=WBrX-iQ9Uao

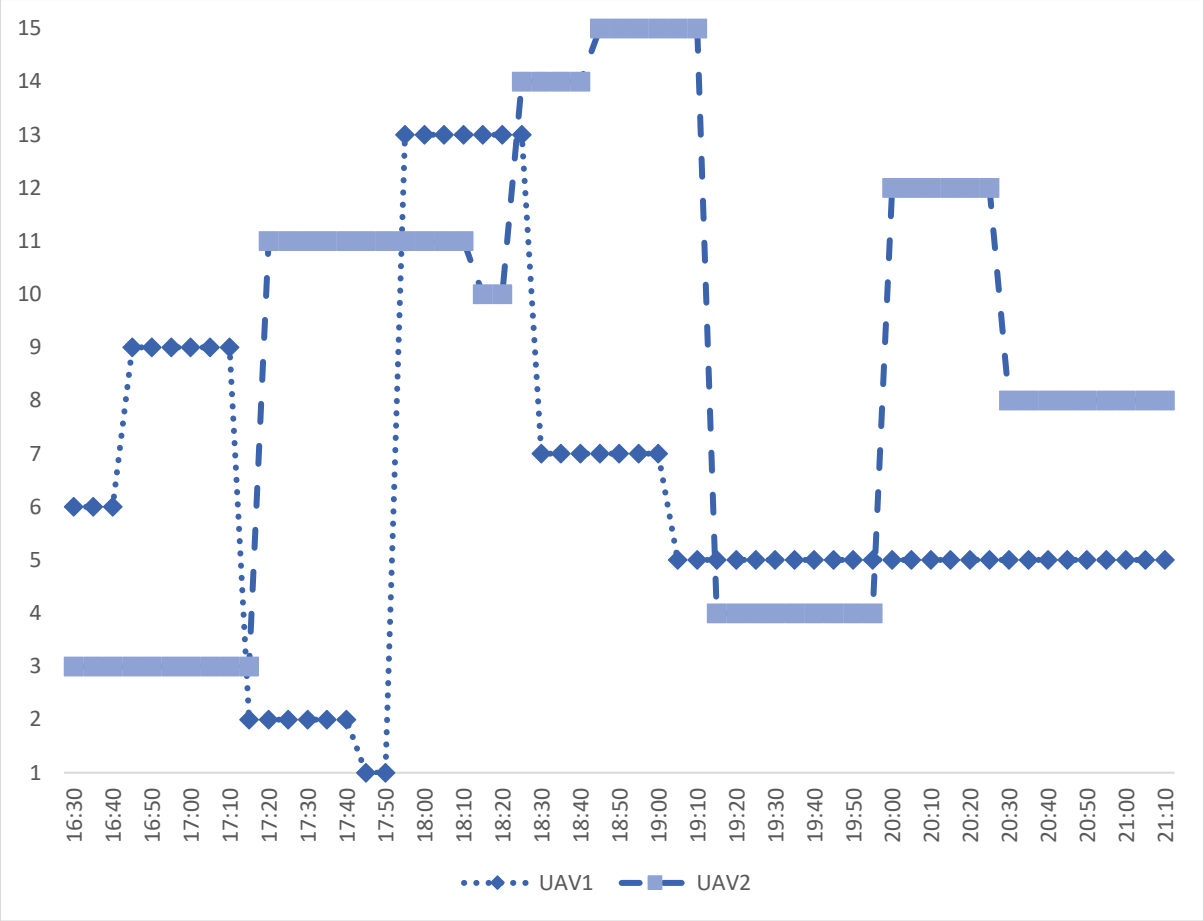

Figure 11: Investigation sequence of the 15 MVs by 2 UAVs.

Figure 12 to Figure 13 shows UAV_1 and UAV_2 cooperating in their investigation of a set of 15 MVs from 16:30 until 17:35.

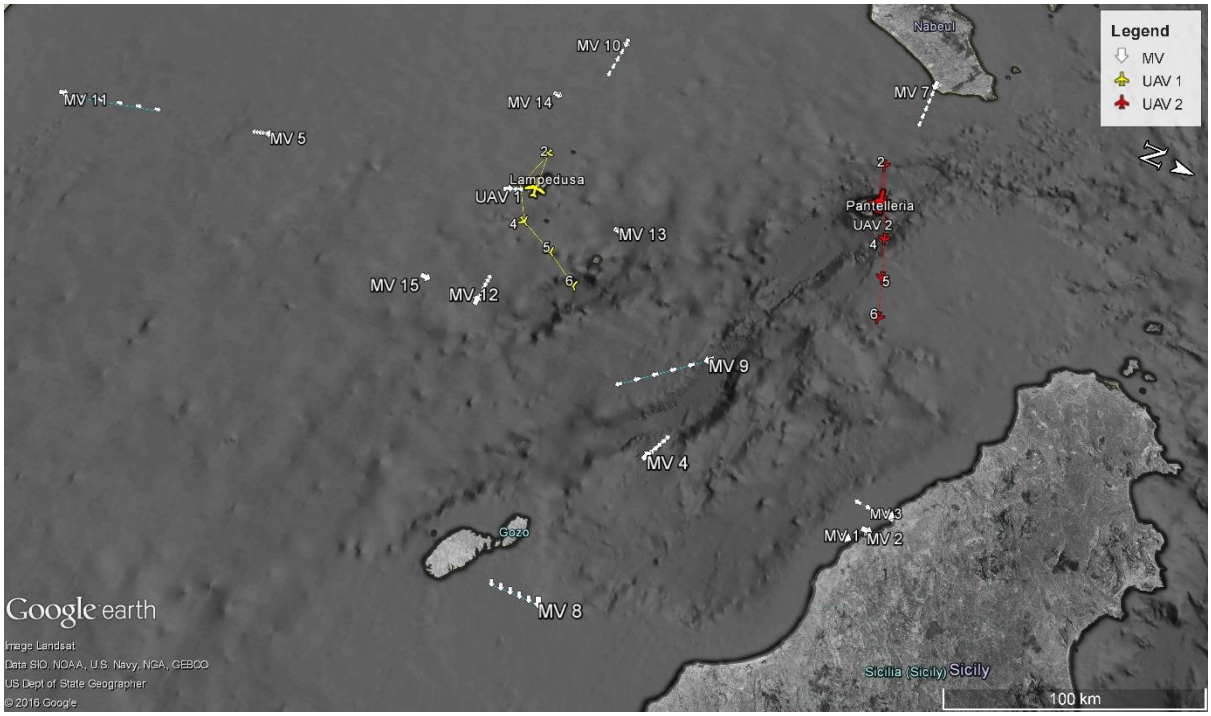

Figure 12: UAV1 and UAV2 in time interval 16:30 – 17:00

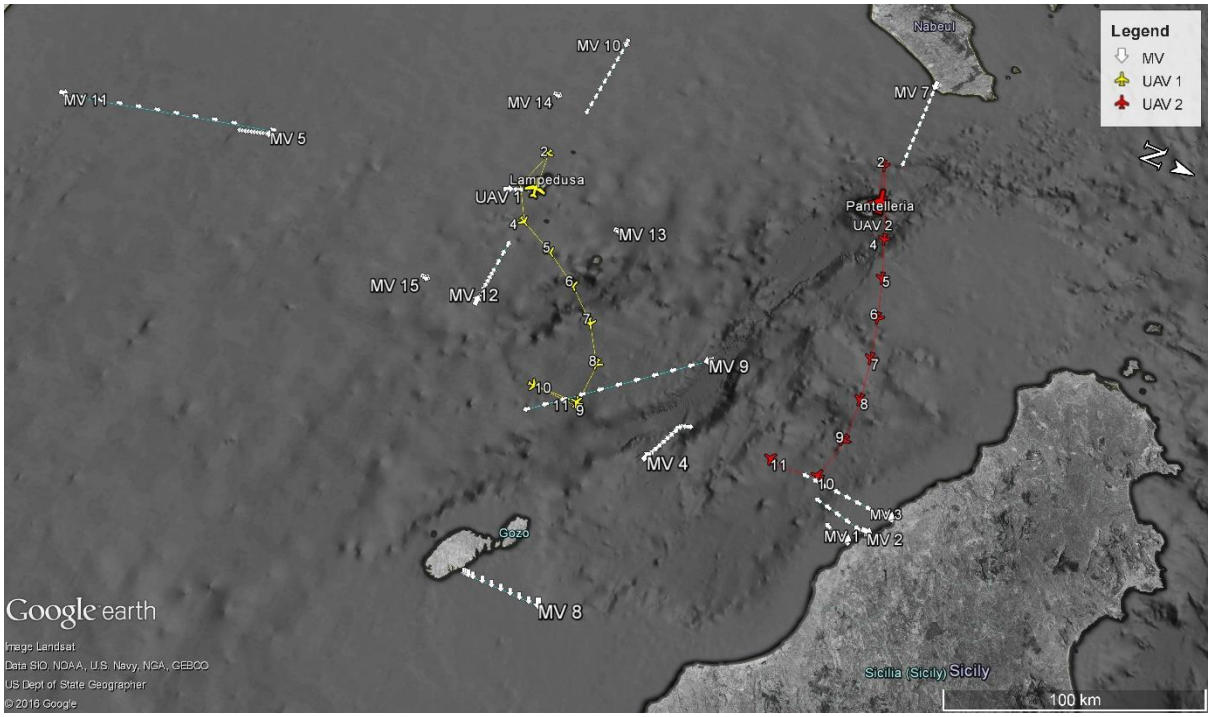

Figure 13: UAV1 and UAV2 in time interval 17:05 – 17:35

The behaviour of the two UAVs can thus be analysed. UAV1 was operating with more important weight for the illegal immigration mission. UAV2 was assigned a higher weight for the drug trafficking mission (Table 4). Figure 12 shows the taking-off of UAVs from

Lampedusa (UAV1) and Pantelleria (UAV2) and their initial routing. For UAV1, MV6 becomes immediately suspicious as it a small speed boat approaching Lampedusa island relatively fast. The distance of UAV to MV is also very short, which makes it the most urgent MV to investigate. It needs 10 minutes (i.e. 16:30 – 16:40) to reach it at camera range. Once the investigation is completed, MV6 is removed from the list of suspicious MV. A PROMETHEE ranking is recalculated at 16:45 and MV9 is found to be the most suspicious MV. It is moving very fast and is not far from the Lampedusa island and the Sicily coast. Therefore, UAV1 adjusts its route to head to MV9. UAV2 has determined that MV3 is the most suspicious because it is very near the coast of Sicily with possible rendezvous with other MVs.

Figure 13 shows that UAV1 has completed to investigate MV9 and it is going to investigate MV2 at 17:15, that is very near to the coast of Sicily and has a possible rendezvous with other MV. In the meantime, UAV2 has completed the investigation of MV3 and is going to investigate MV11, despite the long travel to reach it. MV11 is moving very fast and has a small dimension. If it is not investigated immediately, it will reach Lampedusa and disappear. On the other hand, MV4, a cargo ship that is under suspicion of transferring drug to a speed boat, is investigated late because it is slow and large, which means that it can be located easily at any point of time. MV5 MV12 and MV8 are the last investigated because they are located far off the coast, travelling at very low speed (occasionally remaining stationary) and showing low variation in velocity.

For a single autonomous simulation for a multicriteria (only inspect):

https://www.youtube.com/watch?v=AS4_8Ej0otc

An independent autonomous simulation for a multicriteria (only inspect) with mathematical programming:

https://www.youtube.com/watch?v=OUlg24xKsXI

The swarm autonomous simulation for a single criterion as minimum distance of UAV to MV (inspect and forget) system, can be seen on:

https://www.youtube.com/watch?v=QDSFMPYZdsc

An independent autonomous simulation for a single criterion as minimum distance of UAV to MV (only inspect):

https://www.youtube.com/watch?v=g9nVJTFwnx8

An independent autonomous simulation for a single criterion as minimum distance of UAV to MV (only inspect) with mathematical programming:

https://www.youtube.com/watch?v=tD_EjGqe93w

5. Conclusion

In this paper, we have proposed a decision support system to increase the effectiveness and efficiency of maritime surveillance by means of UAVs. Due to the high complexity and the level of dynamism of the context. Constant re-optimisation may solve the problem, but not efficiently. Therefore, an integrated approach combining AHP, PROMETHEE, GIS and mathematical programming techniques has been proposed. The flexibility of these methods permits their integration into a hybrid model. AHP is used to establish the mission and target weights. This task is done off-line as it is time intensive and may require a debate between the different stakeholders. The reliability of the results is monitored with the consistency measure and used as feed-back mechanism to ensure the quality of the judgements. Once agreed, the weights are used in PROMETHEE to calculate online a ranking of suspicious MV for each UAV. If two (or more) UAVs are assigned to the same MV, a mathematical programming formulation is employed to decide the assignment of the two UAVs by maximizing the sum of the PROMETHEE net flows. Finally, all missions can be viewed on a GIS for a post-analysis.

The fact that once a MV is chosen to be investigated and cannot be unchosen until it has been visited had be discussed in length with the UAV operators. Having the possibility to have a redistribution of UAV to MV at any change could possibly means that a UAV would oscillate between two targets effectively delaying investigation. In our attempt to answer this question,

we have stumbled upon what is a major contribution of our paper. In effect, our algorithm can be used as a routing nearest neighbourhood heuristic methodology by utilizing:

- Multi-Criteria ($C_1 – C_7$) with a distribution of weights.
- Single-Criteria (zeroing the weights of the rest of the criteria), namely the distance UAV to MV (i.e. only C_6)

By varying the investigation and inspection techniques each heuristic methodology can have the following routing "modes":

- Inspect and forget, in which the possibility of two UAVs to investigate same MV is negligible
- Inspect and keep inspecting, in which case which the possibility of two UAVs to investigate same MV is high
- Inspect with mathematical programming (MP), which avoids the possibility of two UAVs to investigate same MV

In summary:

1. Multi-Criteria Inspect & Forget (see Figure 14)
2. Multi-Criteria Inspect (see Figure 15)
3. Multi-Criteria Inspect & MP (see Figure 16)
4. Single-Criteria Inspect & Forget (see Figure 17)
5. Single -Criteria Inspect (see Figure 18)
6. Single -Criteria Inspect & MP (see Figure 19)

Studying Figures 14 – 19, we observe a narrower "focusing effect" on routing with Multi-Criteria compared with Single-Criteria heuristics. Another observation shows only small routing differences between Inspect and Inspect & MP for both heuristics.

This shows the need for measuring flight efficiency for the different routing modes and will be our primary goal for future research.

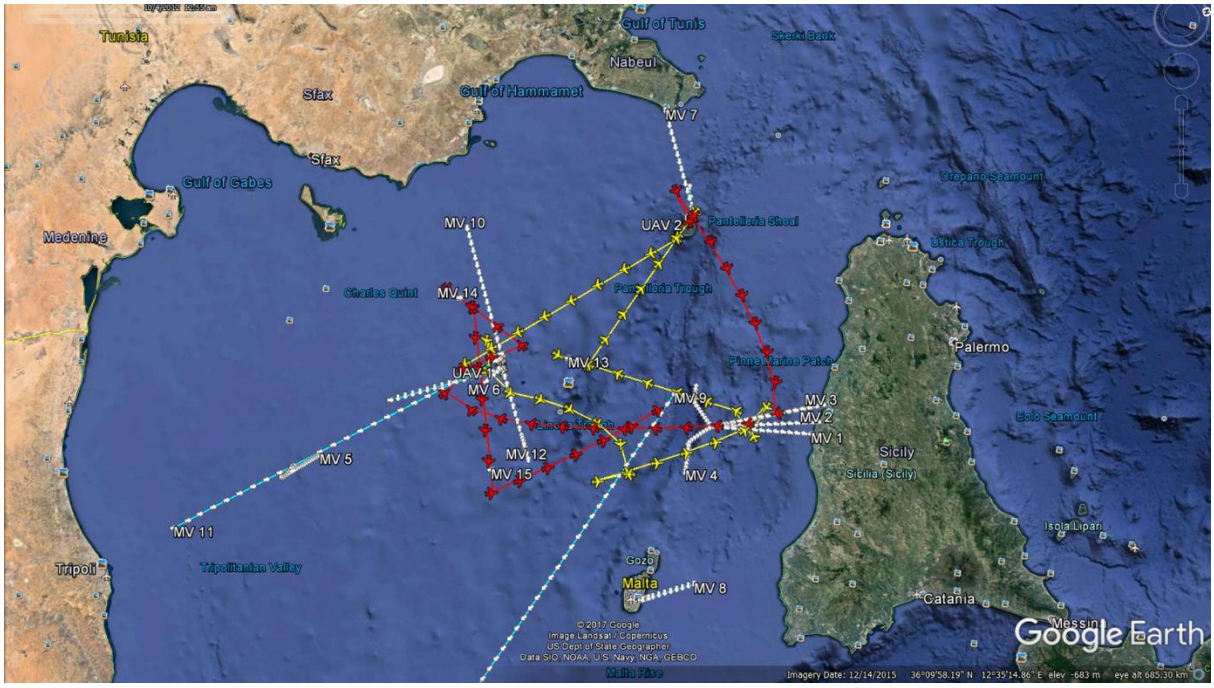

Figure 14. Multi-Criteria Inspect & Forget

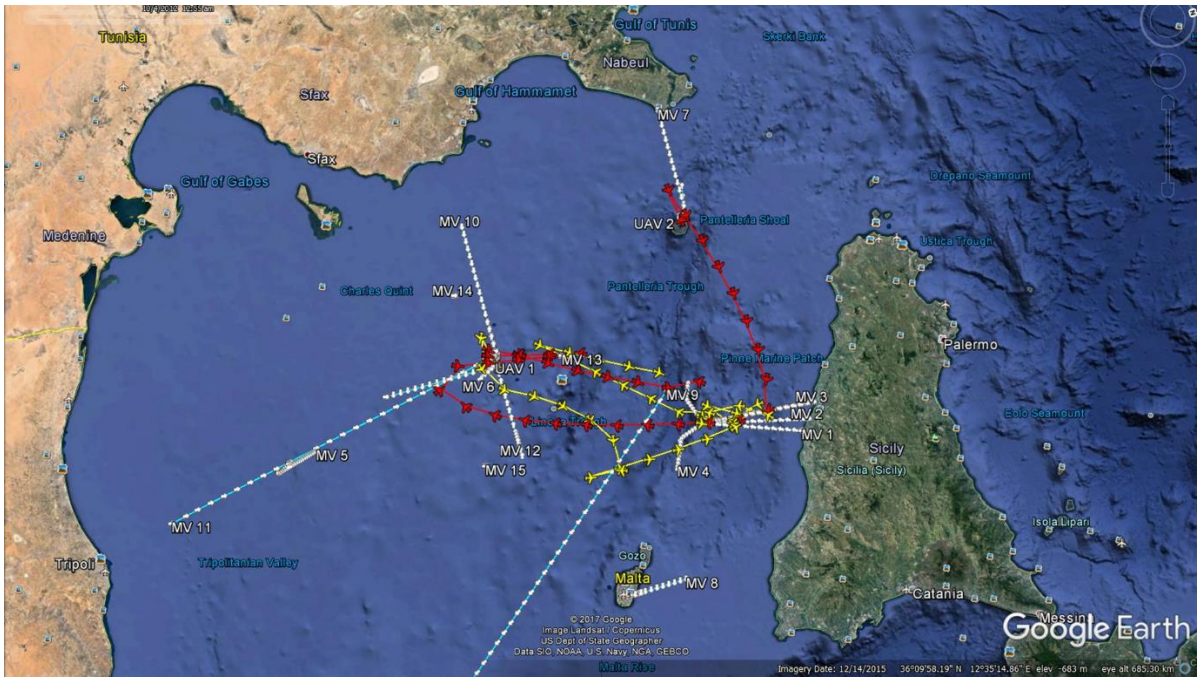

Figure 15. Multi-Criteria Inspect

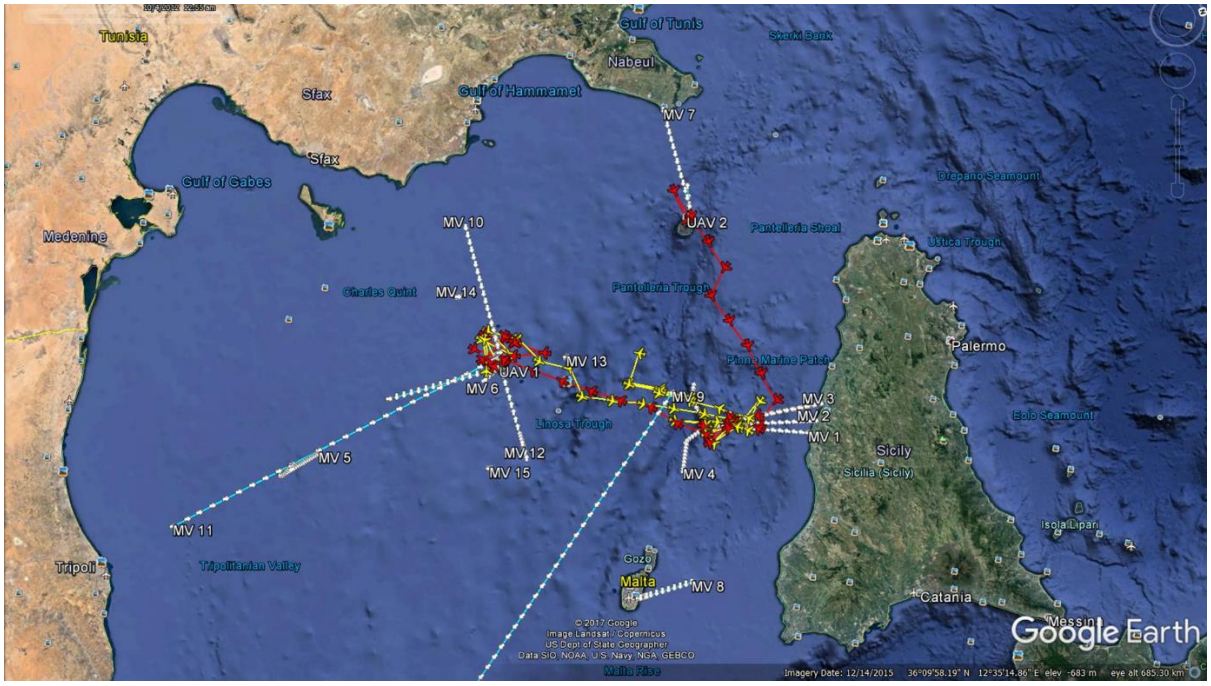

Figure 16. Multi-Criteria Inspect & MP

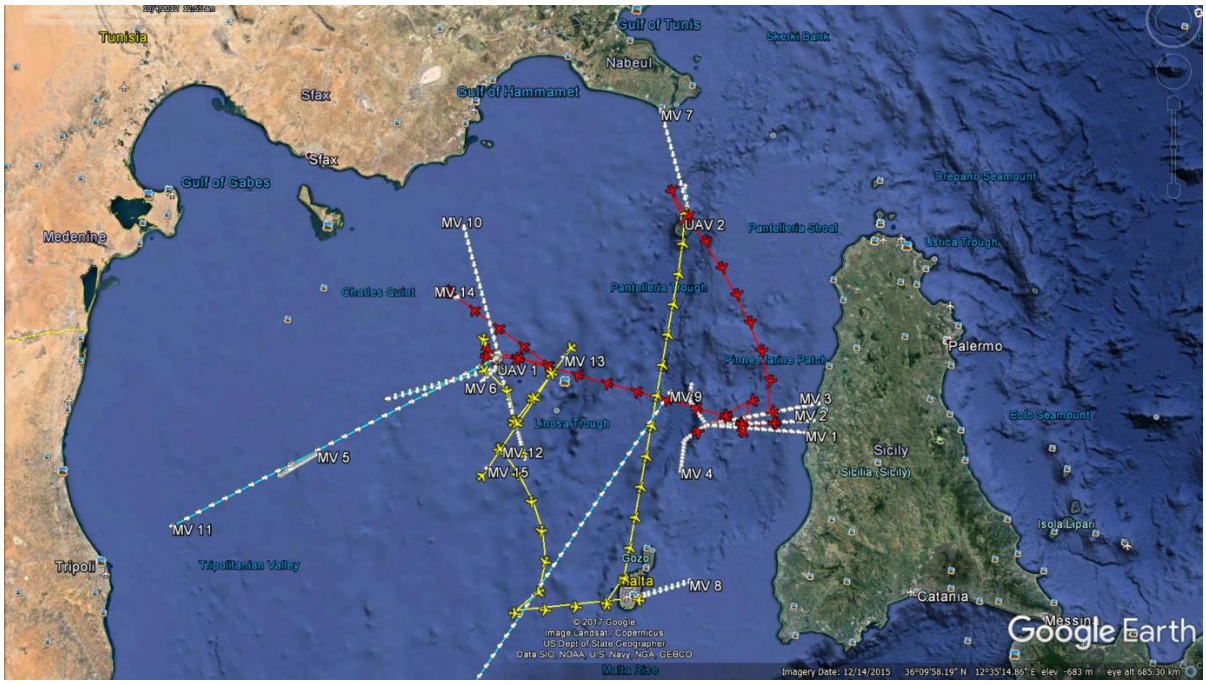

Figure 17. Single-Criteria Inspect & Forget

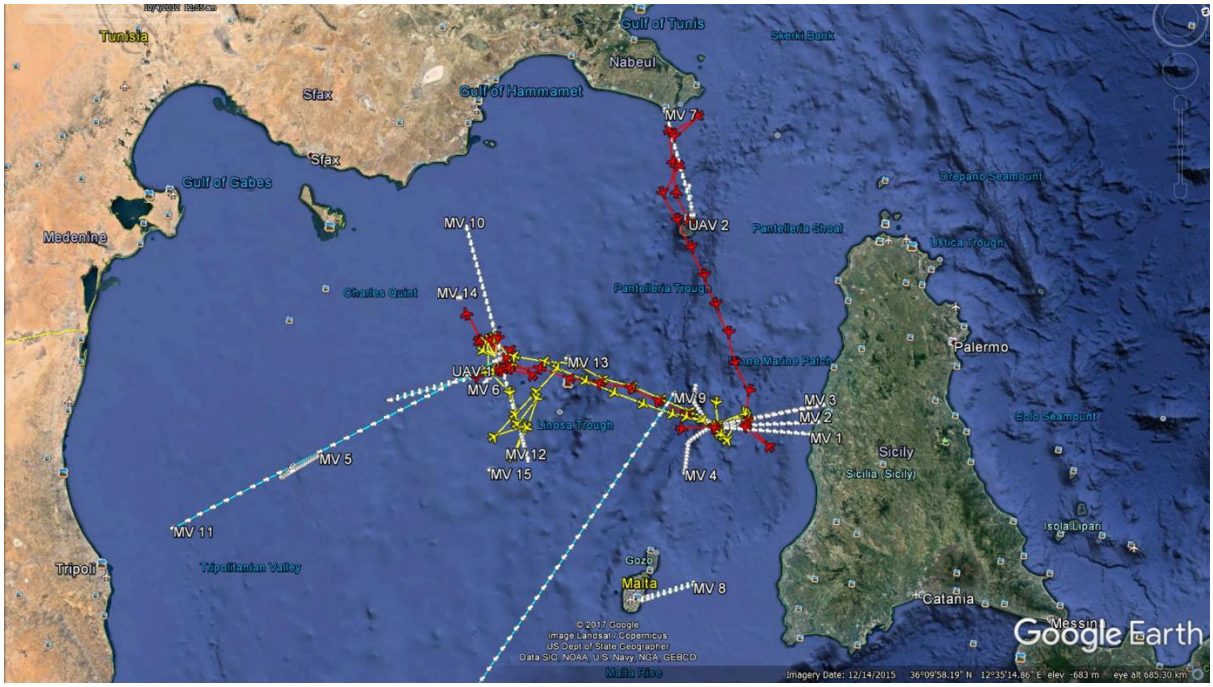

Figure 18. Single -Criteria Inspect

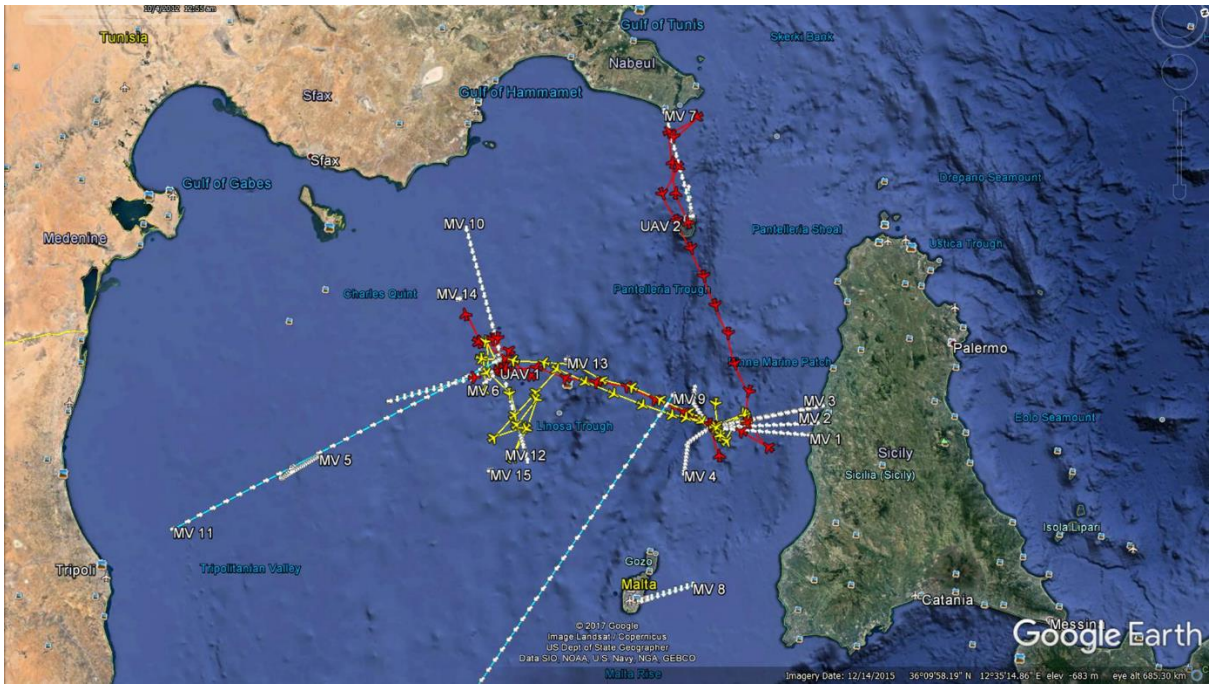

Figure 19. Single -Criteria Inspect & MP

Two operators are needed to remotely control one UAV: one ground control pilot drives the UAV and the second one, the navigator, gives the route to the first one by looking at the MV

and target data they receive. The latter operator could be replaced by the proposed system. Hence, the implementation enables a decrease in the number of operators by providing automated decision support to navigate the UAVs. There are some interesting possibilities should the operators of the MVs become aware of the decision-making processes for directing UAVs. It is not inconceivable that they could 'game' the authorities – for instance, by getting one or two MVs to act in a deliberately "suspicious" manner, and thereby draw the attention of the UAVs. As the UAVs investigate these decoys, their MV colleagues would have a window of opportunity to undertake their nefarious activities in the full knowledge that the UAVs are otherwise occupied for at least a while. In that case, further research would be needed to be carried out to be able to distinguish between genuine suspicious targets and decoy ones. One immediate solution, would be in case a decoy target can be identified, then the next most suspicious target would then take precedence, if the decoys are taking the priority in their suspicion

To the best of our knowledge, a highly dynamic autonomous/semi-autonomous routing problem has not yet been solved. This is our original contribution. The methods used are well-known but their integration to solve this problem is unique. Although our solution has been developed to solve a real problem of defence companies, for the detection of suspicious targets for UAV routing autonomy, this can be generalised to other cases that are set in a highly dynamic environment likewise for unmanned marine vehicle and unmanned land vehicle autonomy. To further improve the system, future research work will investigate the UAVs success rate mission and use this information to feed-back to the system. This analysis can be used to fine tune the weights of the introduced target and mission criteria and depending on the context add or remove one or multiple criteria. In this paper, we assume that a homogeneous fleet of UAVs have the same capacity and can be used in any mission. Another avenue for future research is to consider the capacities of each individual UAV (e.g. sensor capabilities, camera range, night vison, UAV autonomy, etc), select many UAVs from a fleet for the given mission and to design their path mission.

Acknowledgements

This research has been partially funded by the European Commission Seventh Framework Programme with the SeaBILLA grant (241598) [85].

6. References

[1] B. Vergouw, H. Nagel, G. Bondt, and B. Custers, “Drone Technology: Types, Payloads, Applications, Frequency Spectrum Issues and Future Developments,” T.M.C. Asser Press, 2016, pp. 21–45.

[2] International Organization for Standardization, “ISO/TS 15066:2016 - Robots and robotic devices -- Collaborative robots,” *International Organization for Standardization*, 2016. .

[3] D. Floreano and R. J. Wood, “Science, technology and the future of small autonomous drones,” *Nature*, vol. 521, no. 7553, pp. 460–466, May 2015.

[4] Ramser and Dantzig, “the Truck Dispatching Problem *,” *Source Manag. Sci.*, vol. 6, no. 1, pp. 80–91, 1959.

[5] G. Laporte, “Fifty Years of Vehicle Routing,” *Transp. Sci.*, vol. 43, no. 4, pp. 408–416, Nov. 2009.

[6] K. Braekers, K. Ramaekers, and I. Van Nieuwenhuyse, “The vehicle routing problem: State of the art classification and review,” *Computers and Industrial Engineering*, vol. 99. pp. 300–313, 2015.

[7] V. Pillac, M. Gendreau, C. Guéret, and A. L. Medaglia, “A Review of Dynamic Vehicle Routing Problems Bureaux de Montr{é}al : Bureaux de Qu{é}bec,” 2011.

[8] V. Pillac, M. Gendreau, C. Guéret, and A. L. Medaglia, “A Review of Dynamic Vehicle Routing Problems,” *Cirrelt-2011-62*, vol. 225, no. 1, pp. 0–28, 2011.

[9] J. J. Enright, K. Savla, E. Frazzoli, and F. Bullo, “Stochastic and Dynamic Routing Problems for Multiple Uninhabited Aerial Vehicles,” *J. Guid. Control. Dyn.*, vol. 32, no. 4, pp. 1152–1166, Jul. 2009.

[10] M. A. Russell and G. B. Lamont, “A genetic algorithm for unmanned aerial vehicle routing,” *Proc. 2005 Conf. Genet. Evol. Comput. - GECCO ’05*, p. 1523, 2005.

[11] V. K. Shetty, M. Sudit, and R. Nagi, “Priority-based assignment and routing of a fleet of unmanned combat aerial vehicles,” *Comput. {&} Oper. Res.*, vol. 35, no. 6, pp. 1813–1828, Jun. 2008.

[12] S. H. Jacobson, L. A. McLay, S. N. Hall, D. Henderson, and D. E. Vaughan, “Optimal search strategies using simultaneous generalized hill climbing algorithms,” *Math. Comput. Model.*, vol. 43, no. 9, pp. 1061–1073, 2006.

[13] G. W. Kinney, R. R. Hill, and J. T. Moore, “Devising a quick-running heuristic for an unmanned aerial vehicle (UAV) routing system,” *J. Oper. Res. Soc.*, vol. 56, no. 7, pp. 776–786, Jul. 2005.

[14] R. W. Harder, R. R. Hill, and J. T. Moore, “A Java Universal Vehicle Router for Routing Unmanned Aerial Vehicles,” *Int. Trans. Oper. Res.*, vol. 11, no. 3, pp. 259–275, May 2004.

[15] W. Liu, Z. Zheng, and K. Y. Cai, “Bi-level programming based real-time path planning for unmanned aerial vehicles,” *Knowledge-Based Syst.*, vol. 44, pp. 34–47, 2013.

[16] E. Edison and T. Shima, “Integrated task assignment and path optimization for cooperating uninhabited aerial vehicles using genetic algorithms,” *Comput. {&} Oper. Res.*, vol. 38, no. 1, pp. 340–356, Jan. 2011.

[17] Y. Kuroki, G. S. Young, and S. E. Haupt, “UAV navigation by an expert system for contaminant mapping with a genetic algorithm,” *Expert Syst. Appl.*, vol. 37, no. 6, pp. 4687–4697, 2010.

[18] J. J. Ruz, O. Arévalo, G. Pajares, and J. M. De La Cruz, “Decision making among alternative routes for UAVs in dynamic environments,” in *IEEE International Conference on Emerging Technologies and Factory Automation, ETFA*, 2007, pp. 997–1004.

[19] J. Berger, A. Boukhtouta, A. Benmoussa, and O. Kettani, “A new mixed-integer linear programming model for rescue path planning in uncertain adversarial environment,” *Comput. Oper. Res.*, vol. 39, no. 12, pp. 3420–3430, 2012.

[20] H. bin Duan *et al.*, “Max-min adaptive ant colony optimization approach to multi-UAVs coordinated trajectory replanning in dynamic and uncertain environments,” *J. Bionic Eng.*, vol. 6, no. 2, pp. 161–173, 2009.

[21] G. B. Lamont, J. N. Slear, and K. Melendez, “UAV swarm mission planning and routing using multi-objective evolutionary algorithms,” *IEEE Symp. Comput. Intell. Multicriteria Decis. Mak.*, no. Mcdm, pp. 10–20, Apr. 2007.

[22] J. Le Ny, M. Dahleh, and E. Feron, “Multi-UAV dynamic routing with partial observations using restless bandit allocation indices,” in *Proceedings of the American Control Conference*, 2008, pp. 4220–4225.

[23] K. A. Alotaibi, “Unmanned Aerial Vehicle Routing In The Presence Of Threats,” 2014.

[24] C. S. Helvig, G. Robins, and A. Zelikovsky, “The moving-target traveling salesman problem,” *J. Algorithms*, vol. 49, no. 1, pp. 153–174, 2003.

[25] G. Ghiani, F. Guerriero, G. Laporte, and R. Musmanno, “Real-time vehicle routing: Solution concepts, algorithms and parallel computing strategies,” *Eur. J. Oper. Res.*, vol. 151, no. 1, pp. 1–11, 2003.

[26] N. S. Choubey, “Moving Target Travelling Salesman Problem using Genetic Algorithm,” *Int. J. Comput. Appl.*, vol. 70, no. 2, pp. 30–34, 2013.

[27] C. Groba, A. Sartal, X. H. V??zquez, and X. H. Vazquez, “Solving the dynamic traveling salesman problem using a genetic algorithm with trajectory prediction: An application to fish aggregating devices,” *Comput. Oper. Res.*, vol. 56, pp. 22–32, 2015.

[28] D. Perez *et al.*, “Solving the Physical Travelling Salesman Problem: Tree Search and Macro-Actions,” *IEEE Trans. Comput. Intell. AI Games*, vol. 6, no. 1, pp. 31–45, 2014.

[29] M. Mavrovouniotis and S. Yang, “Ant algorithms with immigrants schemes for the dynamic vehicle routing problem,” *Inf. Sci. (Ny).*, vol. 294, pp. 456–477, 2015.

[30] R. J. Kuo, B. S. Wibowo, and F. E. Zulvia, “Application of a fuzzy ant colony system to solve the dynamic vehicle routing problem with uncertain service time,” *Appl. Math. Model.*, vol. 40, no. 23–24, pp. 9990–10001, 2016.

[31] J. Euchi, A. Yassine, and H. Chabchoub, “The dynamic vehicle routing problem: Solution with hybrid metaheuristic approach,” *Swarm Evol. Comput.*, vol. 21, pp. 41–53, 2015.

[32] M. Okulewicz, “Solving Dynamic Vehicle Routing Problem in a continuous search space,” 2016.

[33] M. Okulewicz and J. Mańdziuk, “The impact of particular components of the PSO-based algorithm solving the Dynamic Vehicle Routing Problem,” *Appl. Soft Comput.*, vol. 58, pp. 586–604, 2017.

[34] S. Akpinar, “Hybrid large neighbourhood search algorithm for capacitated vehicle routing problem,” *Expert Syst. Appl.*, vol. 61, pp. 28–38, 2016.

[35] Z. Yang *et al.*, “Dynamic vehicle routing with time windows in theory and practice,” *Nat. Comput.*, vol. 16, no. 1, pp. 119–134, 2017.

[36] F. Furini, C. A. Persiani, and P. Toth, “The Time Dependent Traveling Salesman Planning Problem in Controlled Airspace,” *Transp. Res. Part B Methodol.*, vol. 90, pp. 38–55, 2016.

[37] J. Zak, “The MCDA methodology applied to solve complex transportation decision problems,” *13th Mini-EURO Conf. (Handling Uncertain. Anal. Traffic Transp. Syst.*, pp. 685–693, 2002.

[38] M. Tavana and B. S. . Bourgeois, “A multiple criteria decision support system for autonomous underwater vehicle mission planning and control,” *Int. J. Oper. Res.*, vol. 7, no. 2, pp. 216–239, 2010.

[39] S. Kukadapwar and D. Parbat, “Estimation of Optimal Path on Urban Road Networks Using Ahp Algorithm,” *Int. J. Traffic Transp. Eng.*, vol. 6, no. 1, pp. 13–24, 2016.

[40] S. Bandyopadhyay and R. Bhattacharya, “Finding optimum neighbor for routing based on

multi-criteria, multi-agent and fuzzy approach," *J. Intell. Manuf.*, vol. 26, no. 1, pp. 25–42, 2013.

[41] C. Macharis, J. Springael, K. De Brucker, and A. Verbeke, "PROMETHEE and AHP: The design of operational synergies in multicriteria analysis.," *Eur. J. Oper. Res.*, vol. 153, no. 2, pp. 307–317, Mar. 2004.

[42] W. Ho, "Integrated analytic hierarchy process and its applications - A literature review," *Eur. J. Oper. Res.*, vol. 186, no. 1, pp. 211–228, Apr. 2008.

[43] A. Ishizaka and A. Labib, "A hybrid and integrated approach to evaluate and prevent disasters," *J. Oper. Res. Soc.*, vol. 65, no. 10, pp. 1475–1489, Oct. 2013.

[44] J. Ries and A. Ishizaka, "A multi-criteria support system for dynamic aerial vehicle routing problems," in *CCCA12*, 2012, pp. 1–4.

[45] P. P. Y. Wu, D. Campbell, and T. Merz, "On-board multi-objective mission planning for unmanned aerial vehicles," in *IEEE Aerospace Conference Proceedings*, 2009, pp. 1–10.

[46] S. Jaishankar and R. N. Pralhad, "3D off-line path planning for aerial vehicle using distance transform technique," in *Procedia Computer Science*, 2011, vol. 4, pp. 1306–1315.

[47] Yılmaz Z and Aplak H.S., "Vehicle routing by revaluing the alternative routes by using AHP-TOPSIS Combination," *X. International Logistics {&} Supply Chain Congress 2012 Proceedings, İstanbul, Turkey*. pp. 304–310, 2016.

[48] Y. DEDEMEN, "A MULTI-CRITERIA DECISION ANALYSIS APPROACH TO GIS-BASED ROUTE SELECTION FOR OVERHEAD POWER TRANSMISSION LINES," 2013.

[49] V. K. Saini and V. Kumar, "AHP, fuzzy sets and TOPSIS based reliable route selection for MANET," in *2014 International Conference on Computing for Sustainable Global Development (INDIACom)*, 2014, pp. 24–29.

[50] A. B. Ferreira, M. Costa, A. Tereso, and A. Oliveira, “A Multi-Criteria Decision Support System for a Routing Problem in Waste Collection,” pp. 388–402, 2015.

[51] S. Bandyopadhyay and A. K. Chanda, “A Novel Multi-Criteria Multi-Agent-Based Routing Strategy Based on Tarantula Mating Behavior,” Springer India, 2016, pp. 443–453.

[52] S. Bandni and G. Matrayee, “Routing Strategy based on Tarantula Mating,” *Int. J. Adv. Stud. Comput. Sci. Eng. IJASCSE*, vol. 4, no. 11, 2015.

[53] M. Mavrovouniotis, C. Li, and S. Yang, “A survey of swarm intelligence for dynamic optimization: Algorithms and applications,” *Swarm Evol. Comput.*, vol. 33, no. September 2016, pp. 1–17, 2017.

[54] C. Virágh *et al.*, “Flocking algorithm for autonomous flying robots.,” *Bioinspir. Biomim.*, vol. 9, no. 2, p. 25012, Jun. 2014.

[55] X. Zhu, Z. Liu, and J. Yang, “Model of Collaborative UAV Swarm Toward Coordination and Control Mechanisms Study,” *Procedia Comput. Sci.*, vol. 51, pp. 493–502, 2015.

[56] G. Varela, P. Caamaño, F. Orjales, Á. Deibe, F. López-Peña, and R. J. Duro, “Autonomous UAV based search operations using Constrained Sampling Evolutionary Algorithms,” *Neurocomputing*, vol. 132, pp. 54–67, 2014.

[57] L. Dawson, “Generic Techniques in General Purpose Gpu Programming With Applications To Ant Colony and Image Processing Algorithms,” 2015.

[58] J. Greblicki and M. Walczyński, “Determination of the Optimal Routes for Autonomous Unmanned Aerial Vehicle Under Varying Wind with Using of the Traveling Salesman Problem Algorithm,” in *IFIP International Conference on Computer Information Systems and Industrial Management*, 2016, pp. 334–341.

[59] D. Wu *et al.*, “ADDSEN: Adaptive Data Processing and Dissemination for Drone Swarms in Urban Sensing,” *IEEE Trans. Comput.*, vol. PP, no. 99, p. 1, 2016.

[60] Futurism, “Autonomous Drones are the Future of Urban Security.” 2016.

[61] ROS, “Robot operation system.” 2016.

[62] J. Jackson, G. Ellingson, and T. McLain, “ROSflight: A lightweight, inexpensive MAV research and development tool,” in *International Conference on Unmanned Aircraft Systems (ICUAS)*, 2016, pp. 758–762.

[63] F. Cocchioni, E. Frontoni, G. Ippoliti, S. Longhi, A. Mancini, and P. Zingaretti, “Visual Based Landing for an Unmanned Quadrotor,” *J. Intell. Robot. Syst. Theory Appl.*, vol. 84, no. 1–4, pp. 511–528, Sep. 2015.

[64] A. Benini, M. J. Rutherford, and K. P. Valavanis, “Real-time, GPU-based pose estimation of a UAV for autonomous takeoff and landing,” *Proc. - IEEE Int. Conf. Robot. Autom.*, vol. 2016–June, pp. 3463–3470, 2016.

[65] R. G. Valenti, Y. D. Jian, K. Ni, and J. Xiao, “An autonomous flyer photographer,” in *IEEE International Conference on Cyber Technology in Automation, Control, and Intelligent Systems (CYBER)*, 2016, pp. 273–278.

[66] P. Vivekanandan, G. Garcia, H. Yun, and S. Keshmiri, “A Simplex Architecture for Intelligent and Safe Unmanned Aerial Vehicles,” in *IEEE 22nd International Conference on Embedded and Real-Time Computing Systems and Applications (RTCSA)*, 2016, pp. 69–75.

[67] D. Soto-Gerrero and J.-G. Ramrez-Torres, “A Human-Machine Interface with Unmanned Aerial Vehicles,” in *Robotics and Mechatronics: Proceedings of the 4th IFToMM International Symposium on Robotics and Mechatronics*, S. Zeghloul, M. A. Laribi, and J.-P. Gazeau, Eds. Cham: Springer International Publishing, 2016, pp. 233–242.

[68] New Scientist, “Watch 50 drones controlled at once in a record-breaking swarm.” 2016.

[69] INTEL, “100 Dancing Drones Fly At The Same Time in This Elegant Ballet.” 2016.

[70] Futurism, “Watch Drones Fly so Precisely, They Dance in a Choreographed Light Show.”

2016.

[71] Futurism, “Drones Can Now Perform Hands-On Opertations.” 2016.

[72] T. L. Saaty, “Exploring the interface between hierarchies, multiple objectives and fuzzy sets,” *Fuzzy Sets Syst.*, vol. 1, no. 1, pp. 57–68, 1978.

[73] C. a. Bana e Costa and J.-C. Vansnick, “A critical analysis of the eigenvalue method used to derive priorities in AHP,” *Eur. J. Oper. Res.*, vol. 187, no. 3, pp. 1422–1428, Jun. 2008.

[74] A. Farkas, “The analysis of the principal eigenvector of pairwise comparison matrices,” *Acta Polytech. Hungarica*, 2007.

[75] W.-J. Xu, Y.-C. Dong, and W.-L. Xiao, “Is It Reasonable for Saaty’s Consistency Test in the Pairwise Comparison Method?,” *2008 ISECS Int. Colloq. Comput. Commun. Control. Manag.*, pp. 294–298, 2008.

[76] J. P. Brans and P. H. Vincke, “A PREFERENCE RANKING ORGANIZATION METHOD - (THE PROMETHEE METHOD FOR MULTIPLE CRITERIA DECISION-MAKING),” *Manage. Sci.*, vol. 31, no. 6, pp. 647–656, 1985.

[77] J. Malczewski, “Multiple criteria decision analysis and geographic information systems,” in *Trends in Multiple Criteria Decision Analysis*, Springer, 2010, pp. 369–395.

[78] B. Feizizadeh, P. Jankowski, and T. Blaschke, “A GIS based spatially-explicit sensitivity and uncertainty analysis approach for multi-criteria decision analysis,” *Comput. Geosci.*, vol. 64, pp. 81–95, 2014.

[79] H. Nasiri, A. D. Boloorani, H. A. F. Sabokbar, H. R. Jafari, M. Hamzeh, and Y. Rafii, “Determining the most suitable areas for artificial groundwater recharge via an integrated PROMETHEE II-AHP method in GIS environment (case study: Garabaygan Basin, Iran).,” *Environ. Monit. Assess.*, vol. 185, no. 1, pp. 707–718, Jan. 2013.

[80] E. Xu and H. Zhang, “Spatially-explicit sensitivity analysis for land suitability evaluation,”

Appl. Geogr., vol. 45, pp. 1–9, Dec. 2013.

[81] F. Joerin, M. Thériault, and A. Musy, “Using GIS and outranking multicriteria analysis for land-use suitability assessment,” *Int. J. {…}*, vol. 15, no. 2, pp. 153–174, 2001.

[82] “Earth Point.” p. Tools to convert Excel to KML files.

[83] C. Veness, “Calculate Distance and Bearing between Two Latitude/Longitude Points Using Haversine Formula in JavaScript,” *MIT Open Source*. 2002.

[84] “Home - Leonardo - Aerospace, Defence and Security.” [Online]. Available: http://www.leonardocompany.com/en. [Accessed: 25-Jun-2017].

[85] CORDIS, “SEABILLA,” *FP7-SECURITY*. [Online]. Available: http://cordis.europa.eu/project/rcn/94732_en.html.

7. Appendix

7.1 Criteria (Suspiciousness) calculations

In summary, the suspiciousness of the MVs are calculated with PROMETHEE, based on the following criteria:

1. Dimension of MV

Given by satellite image

2. Change of Speed

a. Calculate distance d travelled in the time interval with (23), where, in equation (24) AOI is replaced by MV_k:

$$\mathrm{a} = \sin^2((\mathrm{lat}_{MV_k(t')} - \mathrm{lat}_{MV_k(t)})/2) + \cos(lat_{MV_k(t')}) * \cos\left(\mathrm{lat}_{MV_{k(t)}}\right) * \sin^2((\mathrm{lon}_{MV_k(t')} - \mathrm{lon}_{MV_k(t)})/2) \quad (26)$$

see discussion in Section 0 for MV speed and positional/intercept prediction.

b. Calculate velocity, v using equation (22)

$$\mathrm{v} = \mathrm{d}/(t' - t) \quad (27)$$

where, *t'* - *t* is the time interval

c. Calculate change in speed by taking the differences of speed at the beginning of the time interval and at the end of it.

3. Rendez-vous

a. Calculate the distance of the MV to the other MVs (23), where, in equation (26) AOI is replaced by MV_k

b. We assume that the one that has the smallest distance with the MV of interest is the most suspicious. Therefore, from a set of MVs, find the minimum distance of the most suspicious MV with its nearest MV.

4. Distance to island

a. Calculate the distance of the MV from Lampedusa (23)

b. Calculate Bearing (21)

c. Calculate Critical Angle (20)

d. Calculate Critical Range (22)

e. Calculate Critical Area (19)

The constants used in our case study are provided by the aviation experts from the department of defence of Italy:

Lampedusa	
β_α	0.4
β_r	0.01
α	30 ◦
range	200 km
latitude	35.515 ◦
longitude	12.580 ◦

5. Distance to coast

a. Calculate the distance of the MV to the Coast of Sicily at Porto di Palma (23)

b. Calculate Bearing (21)

c. Calculate Critical Angle (20)

d. Calculate Critical Range (22)

e. Calculate Critical Area (19)

The constants used in our case study are provided the aviation experts from the department of defence of Italy:

Pantelleria	
β_{α}	0.5
β_{r}	0.1
α	30 ◦
range	250 km
latitude	37.167 ◦
longitude	13.717 ◦

6. Distance UAV to MV

a. Calculate the location (coordinates) of the UAV (10, 11) in the next interval time

b. Calculate the new heading a UAV is required to take for investigating the MV (14)

c. Calculate the distance (sea level) of the UAV defined by equation (17) to most suspicious MV, so that when this distance is < 10 km, the particular most suspicious MV is considered to be investigated and no further action on this MV is required any longer

d. Taking into account the actual flying height of the UAV, calculate the actual distance defined by the Pythagorean equation (18). A more general case may need to take into account curvature of the Earth as to whether UAV has line of sight or obscured by the horizon.

7. MAOC tagging

Is based on an external information received by the operator of the CGC, who decides to flag as highly suspicious a specific MVs.

7.2 UAV1 routing

The complete routing path for *UAV₁* and all the MVs.

UAV_1: ILLEGAL IMMIGRATION				**MV to investigate and its coordinates**				
Time	**lat_{uav}**	**lon_{uav}**	**HDG**	**lat_{MV}**	**lon_{MV}**	**HDG_{uav}**	**$Dist_{uav\_mv}$**	**MV#**
16:30	35.4995	12.6273	260.2839	35.3967	12.6842	155.73	12.54	**6**
16:35	35.4689	12.4096	102.7402	35.4208	12.6692	102.74	24.11	**6**
16:40	35.4291	12.6249	58.5916	35.4450	12.6569	58.59	3.40	**6**
16:45	35.5227	12.8135	28.3120	36.2742	13.3164	28.31	95.05	**9**
16:50	35.6810	12.9186	34.2708	36.2189	13.3736	34.27	72.50	**9**
16:55	35.8295	13.0435	43.0567	36.1636	13.4308	43.06	50.93	**9**
17:00	35.9609	13.1952	57.9803	36.1083	13.4878	57.98	31.00	**9**
17:05	36.0561	13.3838	91.2867	36.0531	13.5447	91.29	14.47	**9**
17:10	36.0518	13.6062	183.9150	35.9978	13.6017	183.92	6.03	**9**
17:15	35.8724	13.5911	359.3418	37.0044	13.5748	359.34	125.88	**2**
17:20	36.0522	13.5885	358.6782	36.9640	13.5622	358.68	101.41	**2**
17:25	36.2321	13.5834	357.7696	36.9235	13.5497	357.77	76.94	**2**
17:30	36.4118	13.5747	356.3598	36.8831	13.5372	356.36	52.51	**2**

17:35	36.5913	13.5605	353.5027	36.8426	13.5247	353.50	28.13	**2**
17:40	36.7700	13.5351	330.3907	36.8022	13.5122	330.39	4.12	**2**
17:45	36.9263	13.4239	130.4235	36.8340	13.5592	130.42	15.82	**1**
17:50	36.8096	13.5949	251.3965	36.7950	13.5409	251.40	5.07	**1**
17:55	36.7520	13.3822	213.5312	35.8981	12.6853	213.53	113.64	**13**
18:00	36.6020	13.2584	213.4572	35.8981	12.6853	213.46	93.64	**13**
18:05	36.4519	13.1351	213.3839	35.8981	12.6853	213.38	73.64	**13**
18:10	36.3016	13.0123	213.3110	35.8981	12.6853	213.31	53.64	**13**
18:15	36.1513	12.8900	213.2387	35.8981	12.6853	213.24	33.64	**13**
18:20	36.0008	12.7681	213.1670	35.8981	12.6853	213.17	13.64	**13**
18:25	35.8501	12.6467	33.0958	35.8981	12.6853	33.10	6.36	**13**
18:30	36.0008	12.7681	320.9628	36.8331	11.9219	320.96	119.57	**7**
18:35	36.1404	12.6278	320.8802	36.8331	11.9219	320.88	99.57	**7**
18:40	36.2798	12.4871	320.7970	36.8331	11.9219	320.80	79.57	**7**
18:45	36.4191	12.3458	320.7133	36.8331	11.9219	320.71	59.57	**7**
18:50	36.5583	12.2040	320.6290	36.8331	11.9219	320.63	39.57	**7**

18:55	36.6972	12.0617	320.5441	36.8331	11.9219	320.54	19.57	**7**
19:00	36.8360	11.9189	140.4586	36.8331	11.9219	140.46	0.43	**7**
19:05	36.6972	12.0617	164.5499	34.1319	12.9169	164.55	295.58	**5**
19:10	36.5238	12.1213	164.6532	34.1439	12.9094	164.65	274.12	**5**
19:15	36.3504	12.1804	164.7622	34.1558	12.9019	164.76	252.66	**5**
19:20	36.1768	12.2390	164.7969	34.1558	12.9019	164.80	232.66	**5**
19:25	36.0032	12.2973	164.8312	34.1558	12.9019	164.83	212.66	**5**
19:30	35.8296	12.3553	164.8652	34.1558	12.9019	164.87	192.66	**5**
19:35	35.6560	12.4131	164.8990	34.1558	12.9019	164.90	172.66	**5**
19:40	35.4823	12.4707	164.9325	34.1558	12.9019	164.93	152.66	**5**
19:45	35.3086	12.5280	164.9657	34.1558	12.9019	164.97	132.66	**5**
19:50	35.1349	12.5850	164.9986	34.1558	12.9019	165.00	112.66	**5**
19:55	34.9612	12.6418	165.0312	34.1558	12.9019	165.03	92.66	**5**
20:00	34.7874	12.6984	165.0635	34.1558	12.9019	165.06	72.66	**5**
20:05	34.6136	12.7547	165.0956	34.1558	12.9019	165.10	52.66	**5**
20:10	34.4398	12.8108	165.1274	34.1558	12.9019	165.13	32.66	**5**

20:15	34.2659	12.8667	165.1589	34.1558	12.9019	165.16	12.66	**5**
20:20	34.0920	12.9223	345.1902	34.1558	12.9019	345.19	7.34	**5**

Mission terminated

7.3 UAV2 routing

The complete routing path for *UAV₂* and all the MVs.

UAV_2 DRUG TRAFFICKING				**MV to investigate and its coordinates**				
Time	**lat_{uav}**	**lon_{uav}**	**HDG**	**lat_{MV}**	**lon_{MV}**	**HDG_{uav}**	**$Dist_{uav\_mv}$**	**MV#**
16:30	36.8005	11.9557	260.2839	37.2637	13.5275	69.27	148.72	**3**
16:35	36.7699	11.7344	70.4339	37.2637	13.5275	70.43	168.40	**3**
16:40	36.8300	11.9461	72.2138	37.2223	13.5226	72.21	146.59	**3**
16:45	36.8847	12.1602	74.3111	37.1808	13.5177	74.31	124.91	**3**
16:50	36.9332	12.3769	76.8516	37.1393	13.5128	76.85	103.40	**3**
16:55	36.9739	12.5961	80.0652	37.0978	13.5080	80.07	82.10	**3**
17:00	37.0047	12.8180	84.4062	37.0563	13.5031	84.41	61.09	**3**
17:05	37.0220	13.0422	91.0014	37.0148	13.4983	91.00	40.50	**3**
17:10	37.0187	13.2674	104.0458	36.9733	13.4934	104.05	20.69	**3**
17:15	36.9748	13.4858	177.0362	36.9319	13.4886	177.04	4.78	**3**
17:20	36.7952	13.4974	192.3737	34.3381	12.8453	192.37	279.52	**11**
17:25	36.6195	13.4494	193.2500	34.4261	12.8239	193.25	250.38	**11**
17:30	36.4444	13.3982	194.2797	34.5142	12.8025	194.28	221.31	**11**

17:35	36.2701	13.3431	195.5305	34.6022	12.7806	195.53	192.33	**11**
17:40	36.0968	13.2835	197.0658	34.6903	12.7589	197.07	163.47	**11**
17:45	35.9248	13.2184	199.0345	34.7783	12.7372	199.03	134.74	**11**
17:50	35.7548	13.1461	201.7010	34.8664	12.7156	201.70	106.23	**11**
17:55	35.5876	13.0643	205.6358	34.9544	12.6939	205.64	78.02	**11**
18:00	35.4254	12.9688	212.4022	35.0425	12.6722	212.40	50.38	**11**
18:05	35.2735	12.8507	228.9826	35.1306	12.6500	228.98	24.19	**11**
18:10	35.1554	12.6847	323.7919	35.2186	12.6281	323.79	8.72	**11**
18:15	35.3004	12.5546	353.5515	35.5253	12.5233	353.55	25.16	**10**
18:20	35.4791	12.5298	353.5372	35.5253	12.5233	353.54	5.16	**10**
18:25	35.6579	12.5048	232.8116	35.3767	12.0517	232.81	51.57	**14**
18:30	35.5490	12.3287	232.7091	35.3767	12.0517	232.71	31.57	**14**
18:35	35.4399	12.1531	232.6071	35.3767	12.0517	232.61	11.57	**14**
18:40	35.3306	11.9779	52.5057	35.3767	12.0517	52.51	8.43	**14**
18:45	35.4399	12.1531	99.1698	35.2825	13.3061	99.17	106.01	**15**
18:50	35.4111	12.3710	99.2961	35.2825	13.3061	99.30	86.01	**15**

18:55	35.3818	12.5887	99.4222	35.2825	13.3061	99.42	66.01	**15**
19:00	35.3522	12.8062	99.5481	35.2825	13.3061	99.55	46.01	**15**
19:05	35.3221	13.0236	99.6739	35.2825	13.3061	99.67	26.01	**15**
19:10	35.2917	13.2408	99.7994	35.2825	13.3061	99.80	6.01	**15**
19:15	35.2609	13.4579	352.7779	36.5422	13.2558	352.78	143.63	**4**
19:20	35.4393	13.4302	351.7521	36.5403	13.2315	351.75	123.72	**4**
19:25	35.6173	13.3984	350.6596	36.5487	13.2077	350.66	104.97	**4**
19:30	35.7948	13.3624	349.3462	36.5570	13.1839	349.35	86.25	**4**
19:35	35.9716	13.3213	349.3221	36.5570	13.1839	349.32	66.25	**4**
19:40	36.1483	13.2801	344.8244	36.5736	13.1364	344.82	49.01	**4**
19:45	36.3219	13.2216	341.3942	36.5819	13.1126	341.39	30.51	**4**
19:50	36.4923	13.1502	333.2503	36.5902	13.0888	333.25	12.19	**4**
19:55	36.6529	13.0493	166.9834	36.5985	13.0650	166.98	6.21	**4**
20:00	36.4777	13.0997	201.7197	35.5094	12.6264	201.72	115.78	**12**
20:05	36.3105	13.0171	201.4744	35.5094	12.6303	201.47	95.65	**12**
20:10	36.1431	12.9356	194.0485	35.5094	12.7408	194.05	72.62	**12**

20:15	35.9686	12.8816	188.6209	35.5094	12.7961	188.62	51.64	**12**
20:20	35.7908	12.8484	179.5029	35.5094	12.8514	179.50	31.29	**12**
20:25	35.6109	12.8503	179.5041	35.5094	12.8514	179.5041	11.29	12
20:30	35.4311	12.8522	359.5052	35.5094	12.8514	-0.4948	8.71	8
20:35	35.6109	12.8503	250.4185	35.3767	12.0517	-109.5815	76.85	8
20:40	35.5505	12.6420	76.0425	35.9119	14.5092	76.0425	173.26	8
20:45	35.5937	12.8567	76.1673	35.9119	14.5092	76.1673	153.26	8
20:50	35.6365	13.0716	76.2925	35.9119	14.5092	76.2925	133.26	8
20:55	35.6789	13.2867	76.4179	35.9119	14.5092	76.4179	113.26	8
21:00	35.7210	13.5020	76.5435	35.9119	14.5092	76.5435	93.26	8
21:10	35.7626	13.7176	76.6695	35.9119	14.5092	76.6695	73.26	8
21:15	35.8039	13.9334	76.7956	35.9119	14.5092	76.7956	53.26	8